*Netadis Summer School*

# Random Graphs & Random Maps: Statistical Physics Approaches to Static and Dynamical Properties

R. Monasson, LPT-ENS, Paris

Netadis Summer School on Complex Systems, Hillerod, September 2013

# Overview of lectures

- Random Graphs: Typical and Rare Properties
- Random Graphs: Dynamical Processes and Replica Method
- Random Spatial Maps: Spin Glass Models for Static and Dynamical Properties

- Exercises: today and tomorrow

- Solutions, lecture notes & further readings:

  http://www.lpt.ens.fr/~monasson/Netadis/index.html

- Please let me know if you find mistakes in the notes …

# Today

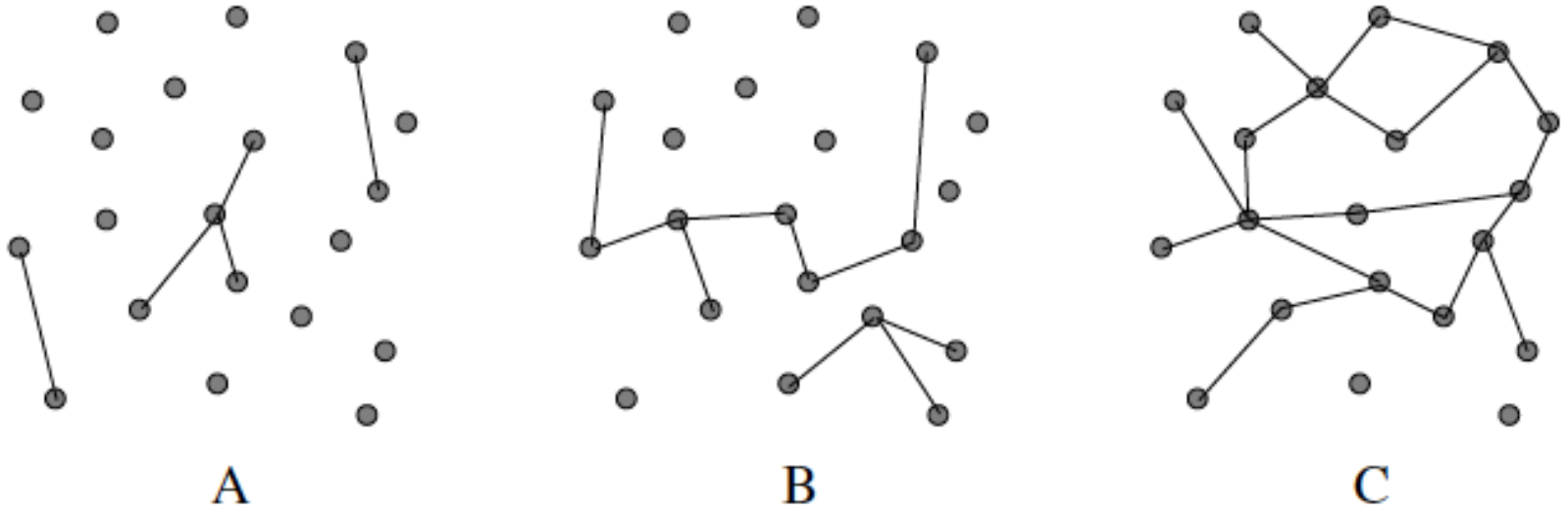


FIG. 1.1. Examples of random graphs generated at fixed number $N_E$ of edges (Distribution I). All graph include $N = 20$ vertices (grey dots). The average degrees of valency, $c = 2N_E/N$, equal $c = 0.5$ (**A**), $c = 1$ (**B**), and $c = 2$ (**C**). The labels of the vertices have been permuted to obtain planar graphs, *i.e.* avoid crossing of edges.

# Trees on V vertices

Cayley theorem (1889)

Nb. of trees = $V^{V-2}$

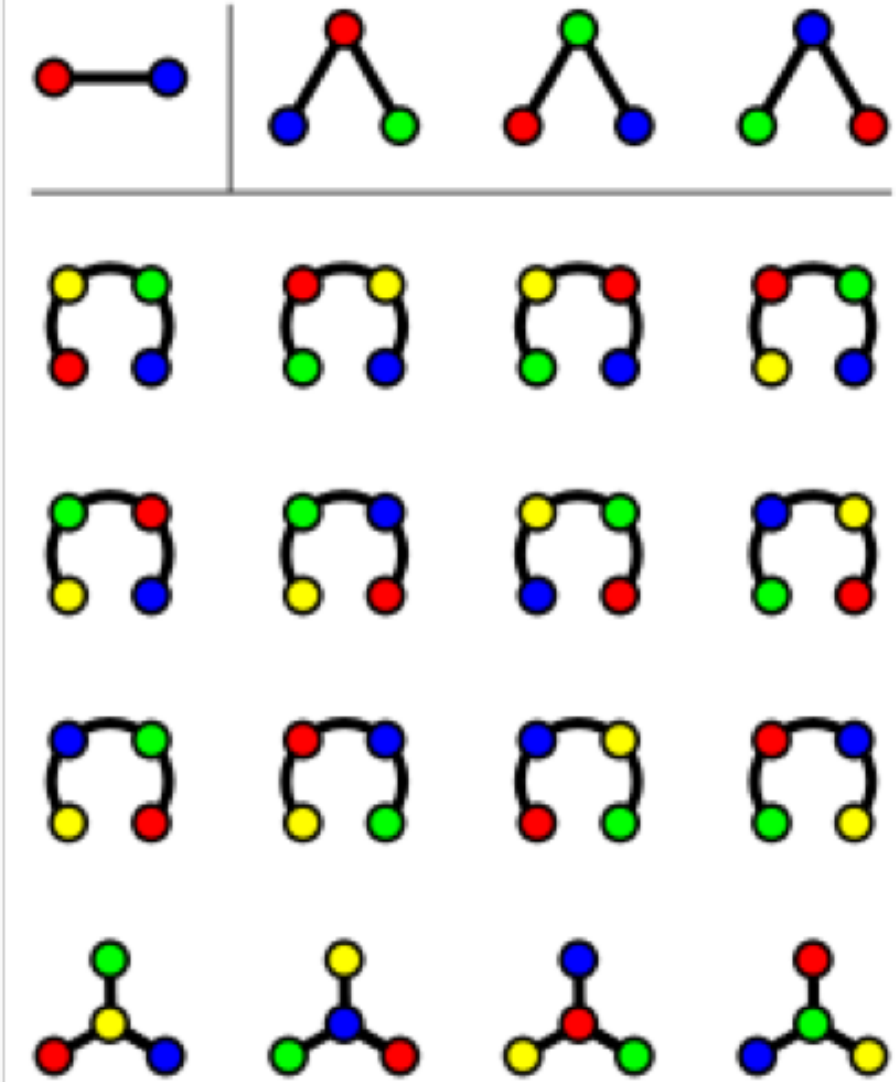

Cayley's formula implies that there is $1 = 2^{2-2}$ tree on two vertices, $3 = 3^{3-2}$ trees on three vertices, and $16 = 4^{4-2}$ trees on four vertices.

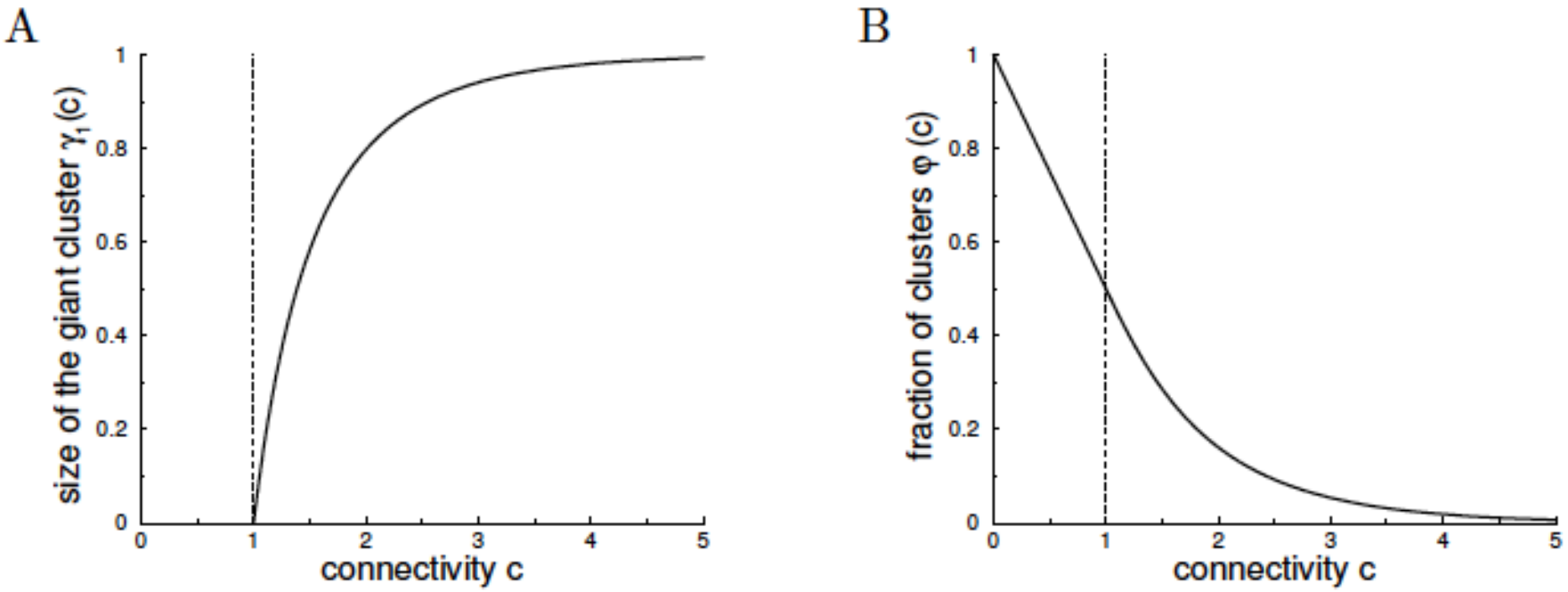


FIG. 1.2. The percolation transition in the random graph. Fraction $\gamma_1(c)$ of vertices in the largest component (**A**), and number $\varphi^*(c)$ of clusters per vertex (**B**) a function of the average connectivity $c$ of the random graph. The vertical dot–dashed line $c = 1$ indicates the location of the percolation threshold.

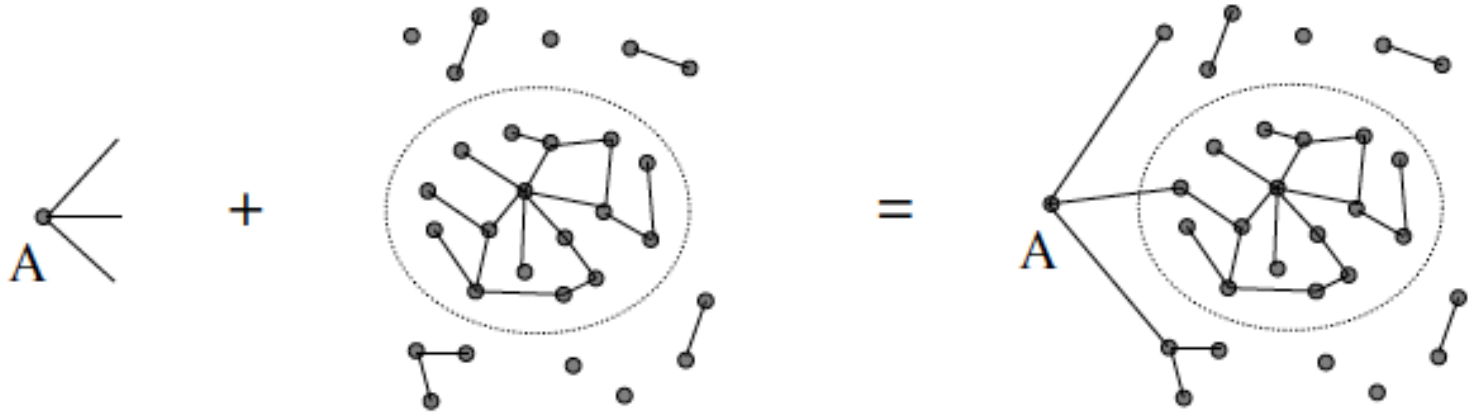


FIG. 1.3. Addition process of one vertex $A$ and its $v = 3$ edges to a random graph $G$. Prior to merging, $G$ is made of isolated nodes, small connected components, and a giant component (surrounded by the dotted line). After merging, the new vertex belongs to the giant component.

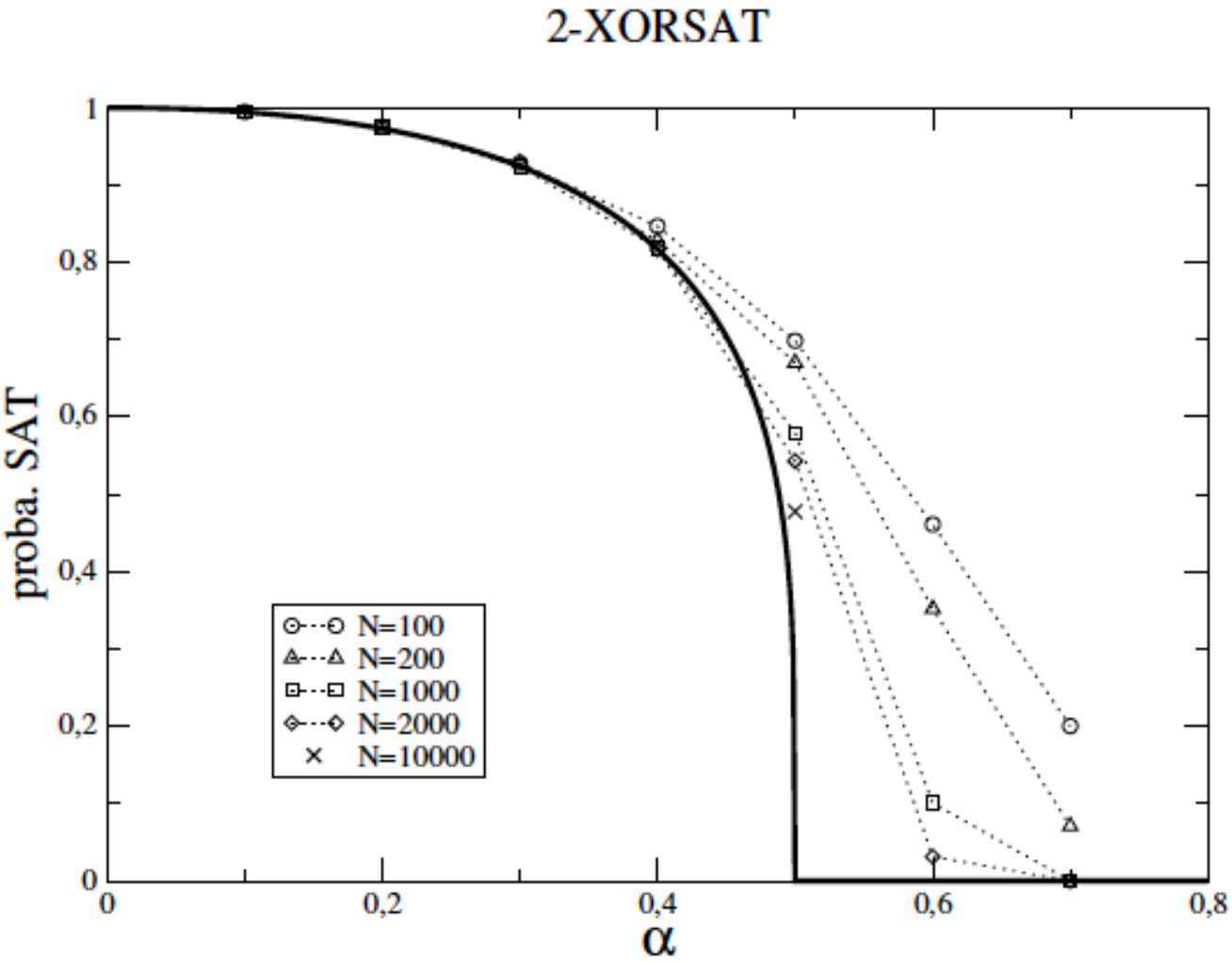


FIG. 1.4. Probability that a random 2-XORSAT formula is satisfiable as a function of the ratio $\alpha$ of equations per variable, and for various sizes $N$. The full line is the asymptotic analytical formula (1.26).

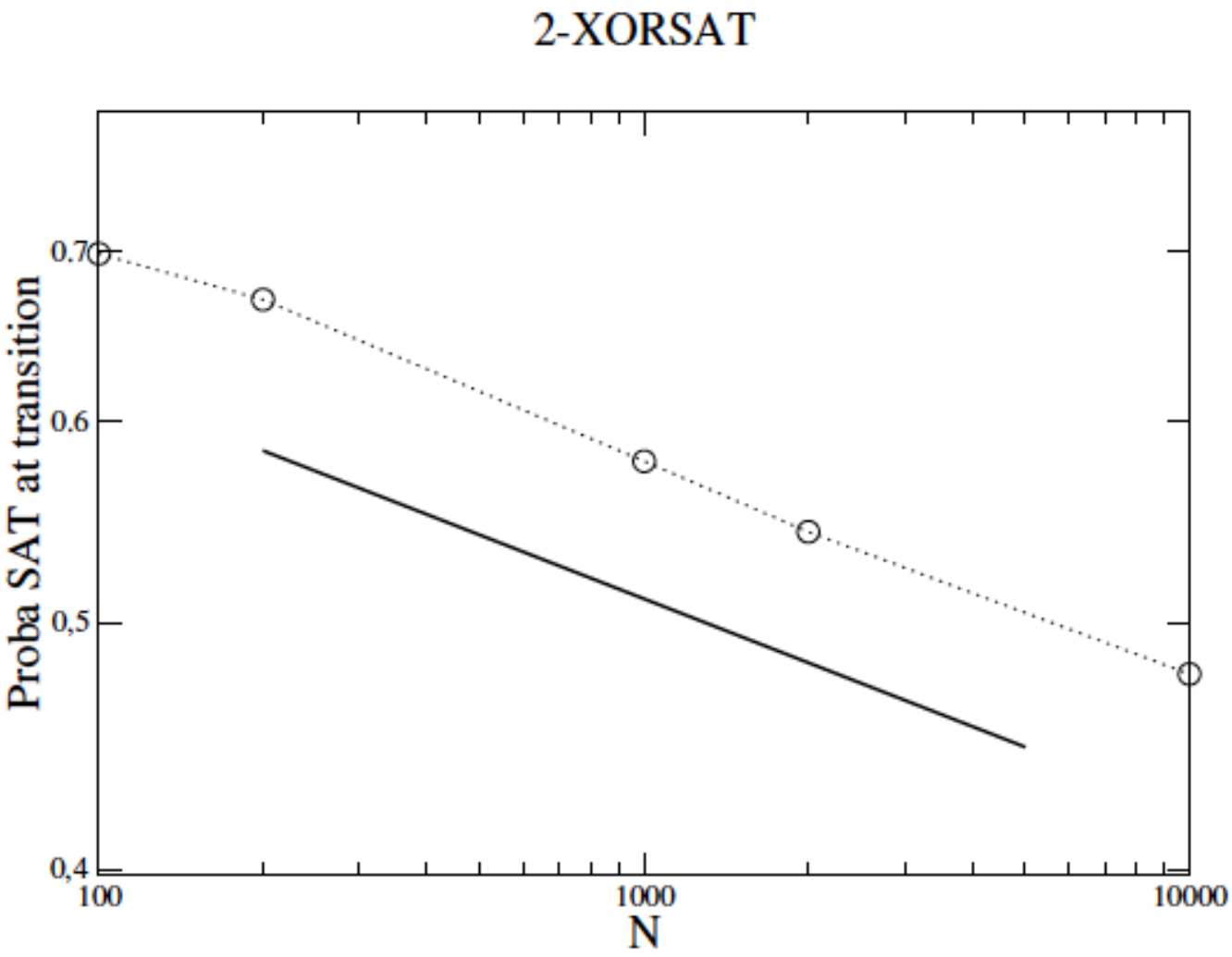


FIG. 1.5. $P_{SAT}$ as a function of the size $N$ at the Sat/Unsat ratio for 2-XORSAT in log-log plot. The slope $-\frac{1}{12}$ (1.27) is shown for comparison.

# Large deviation function for nb of connected components

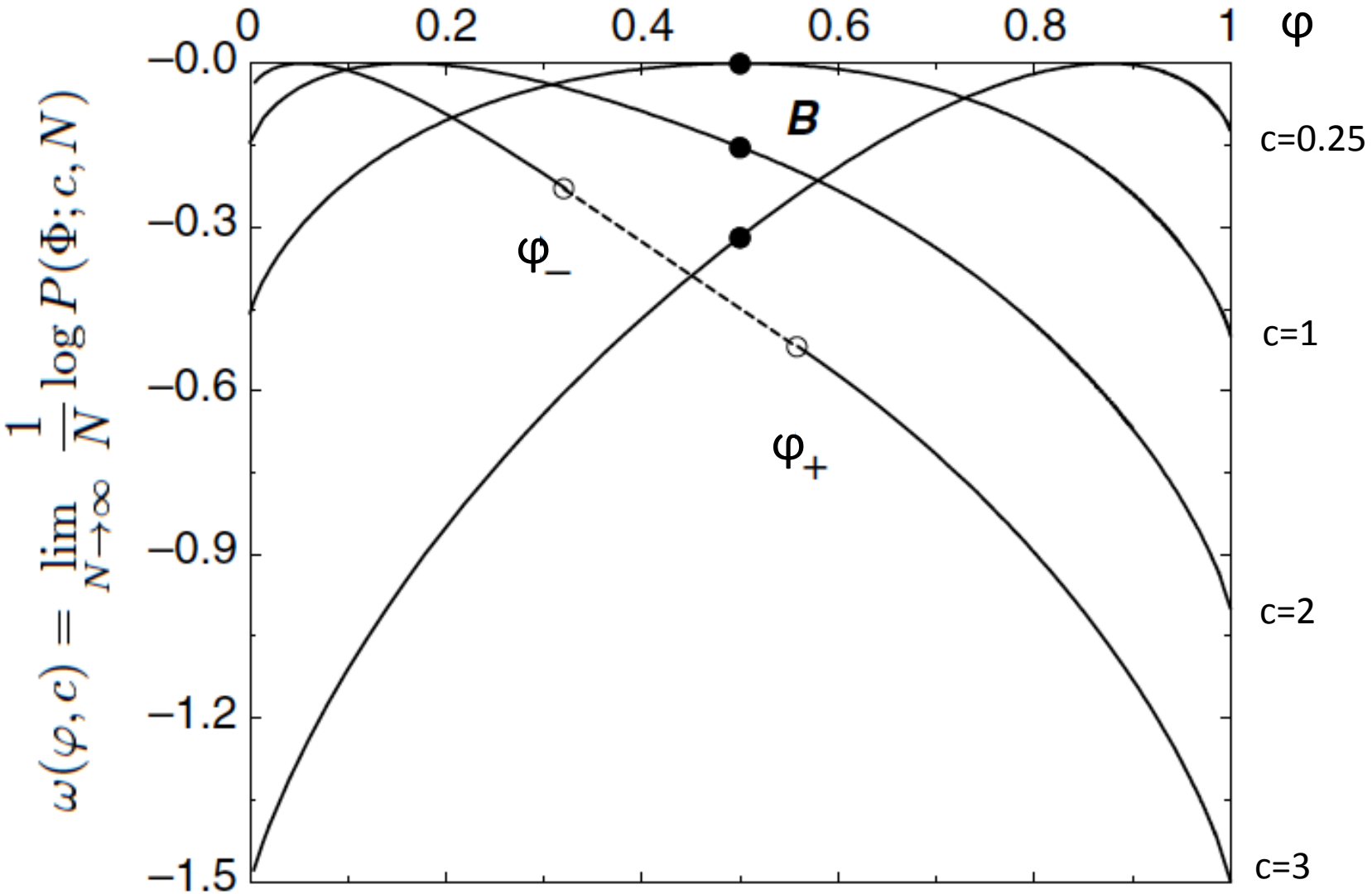

# Large deviation function for nb of connected components (Monte Carlo simulations)

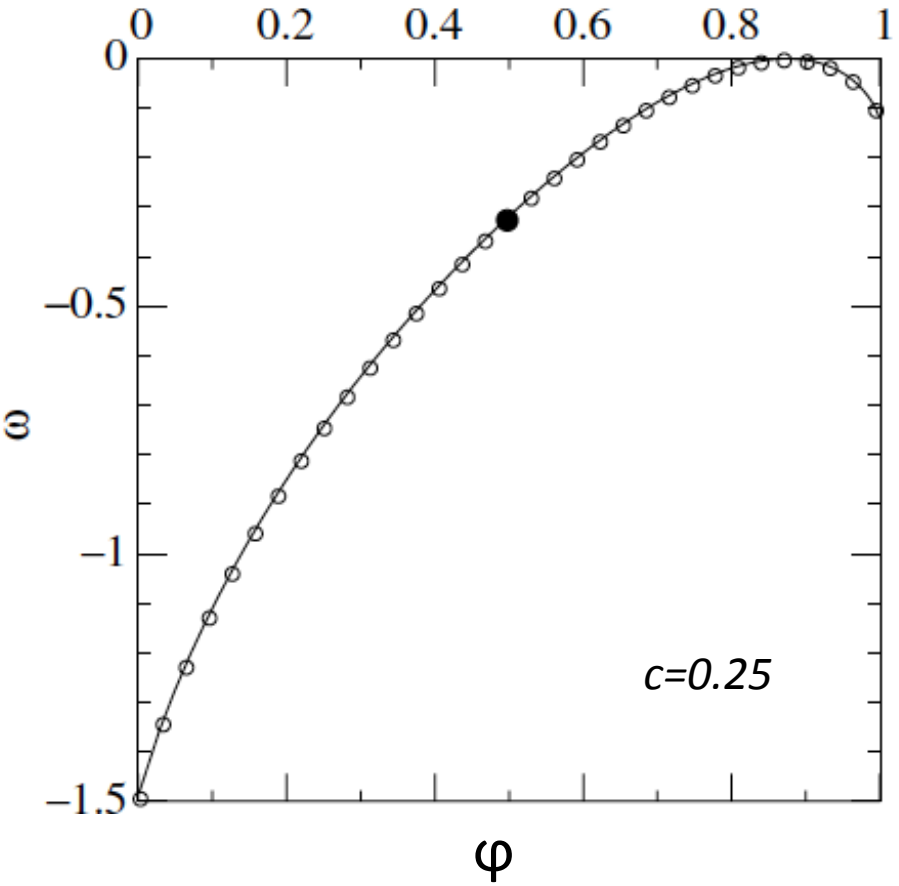


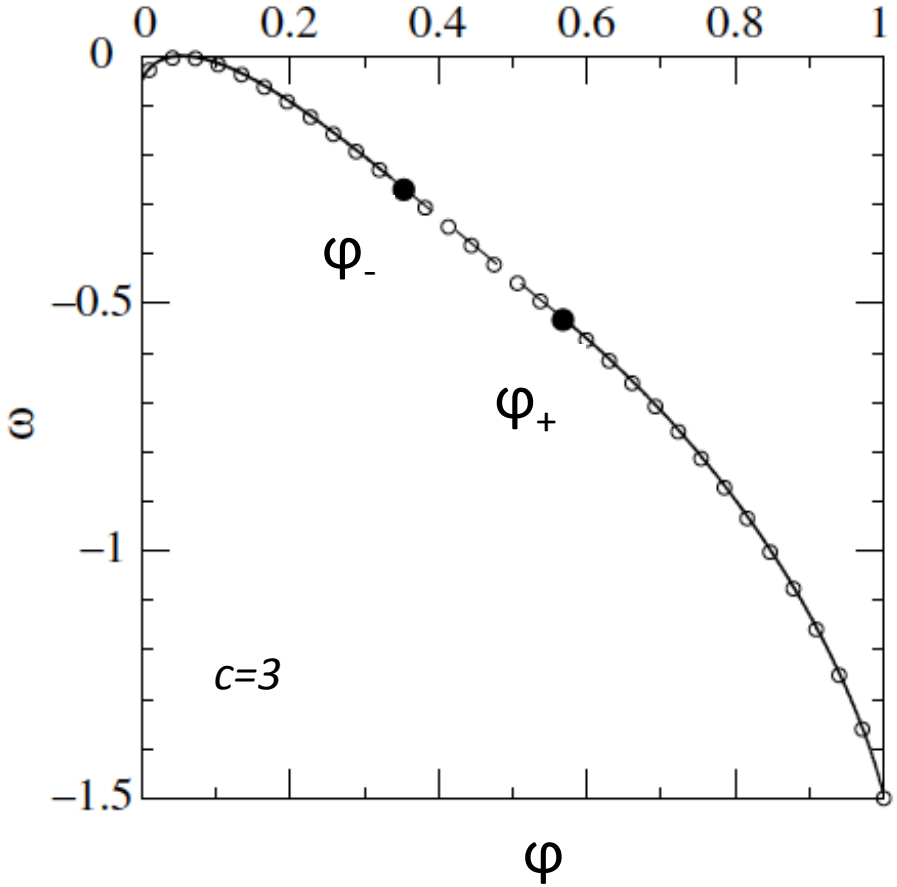

# Exercise:

Consider the random 1-XORSAT model with $N$ variables, and ratio $\alpha$ of clauses per variables.

1. Show that the critical value of the ratio above which the probability of satisfaction vanishes when $N \to \infty$ is $\alpha_c = 0$.

2. Show that, for $\alpha > 0$, there exists a strictly positive rate function defined through

$$\lim_{N\to\infty} \frac{1}{N} \log P_{SAT}(N, \alpha) = -\omega(\alpha) \ .$$

Calculate $\omega(\alpha)$ in the fixed-size ensemble, and then in the fixed-probability ensemble.

**Yesterday:**

Random graphs: typical & rare properties of structure
(nb, size, nature of components, cycles, …)

**Today**

Interacting models on random graphs (phase transitions)
with 2 approaches:

- Modeling of dynamical changes of a graph (cf. N. Wormald's paper)

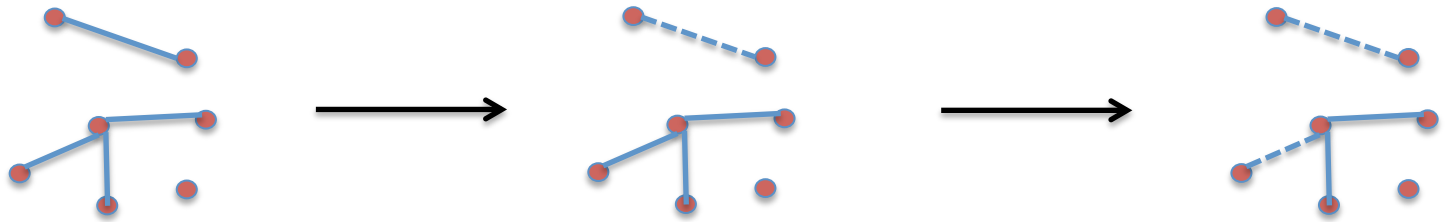

- Replica method (spin glasses, RMT, …)

Illustration of general techniques on a particular case:
Random sets of Boolean equations with 3 variables each

$$x_1+x_5+x_7=0,\ x_1+x_2+x_4=1,\ \ldots,\ x_5+x_8+x_{11}=0$$

Why?

1. Calculations can be done exactly and (rather) easily

2. Paradigm of spin glass model on random (hyper)graphs

3. Interesting from a computational point of view
   (Approximation theory)

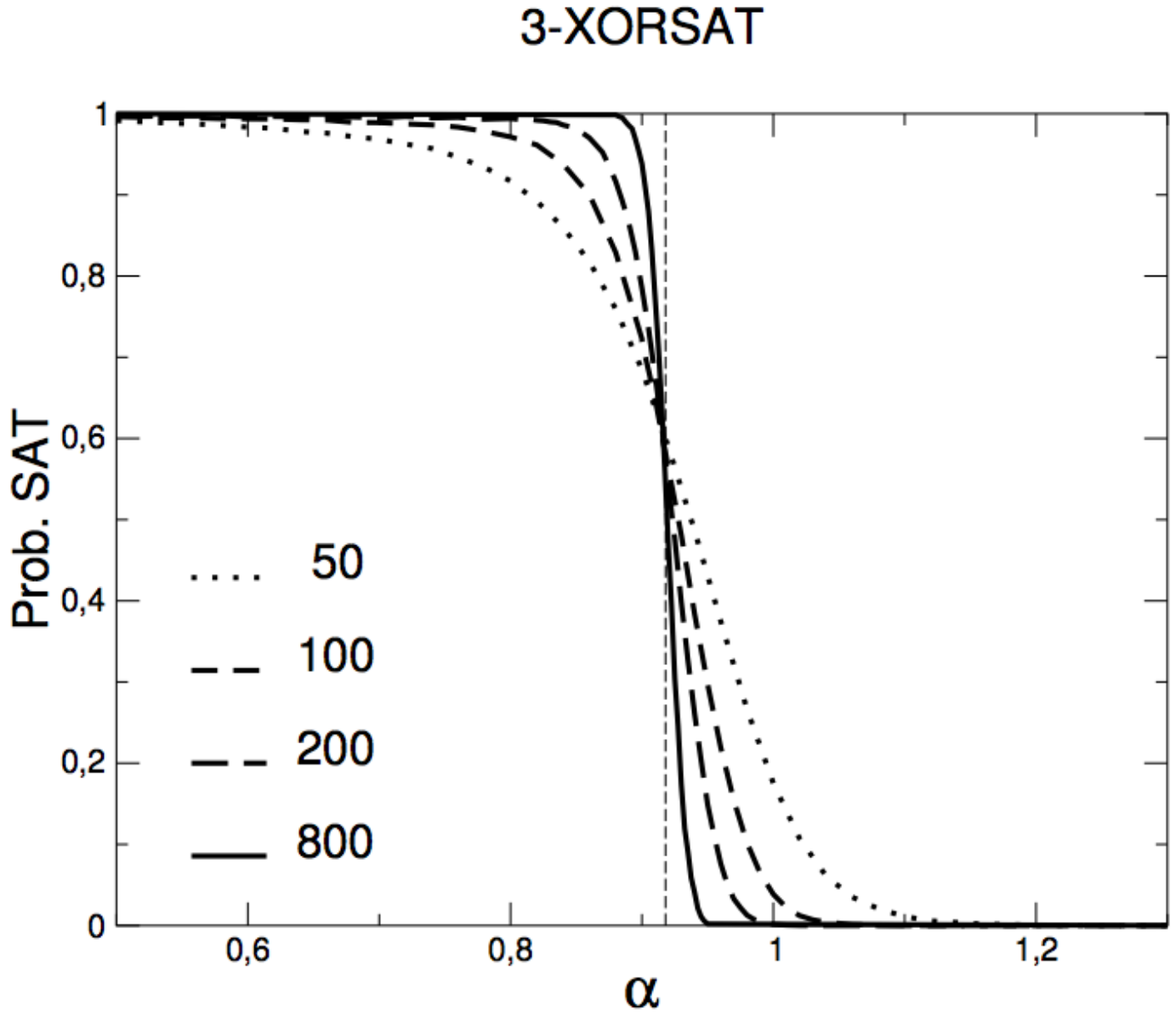
3-XORSAT
Prob. SAT
1
0,8
0,6
0,4
0,2
0
0,6
0,8
1
1,2
α
50
100
200
800

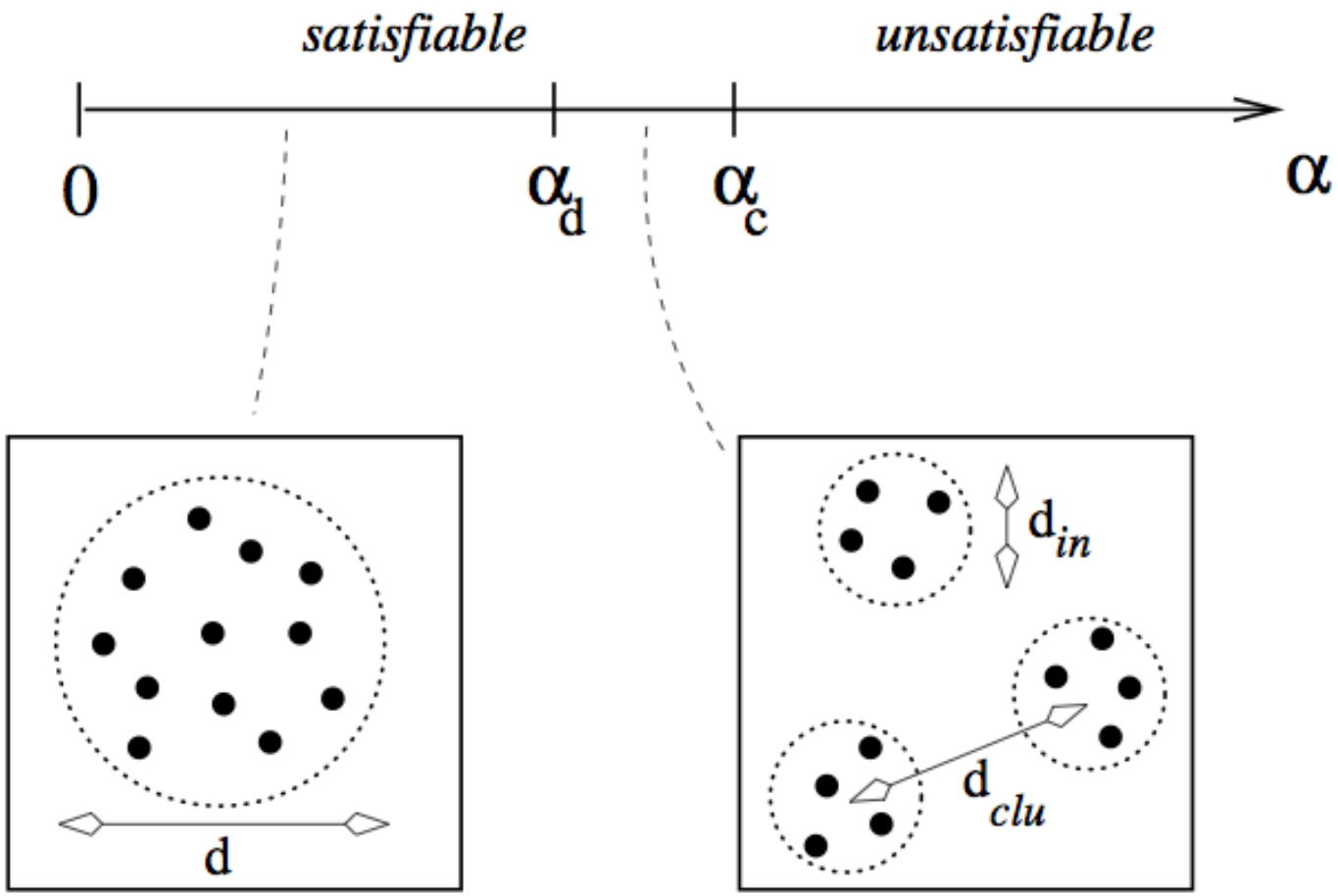


FIG. 2.4. Phase diagram of 3-XORSAT. A 'geometrical' phase transition takes place in the satisfiable phase at $\alpha_d \simeq 0.818$. At small ratios $\alpha < \alpha_d$ solutions are uniformely scattered on the $N$-dimensional hypercube, with a typical normalized Hamming distance $d = \frac{1}{2}$. At $\alpha_d$ the solution space discontinuously breaks into disjoint clusters: the Hamming distance $d_{in} \simeq 0.14$ between solutions inside a cluster is much smaller than the typical distance $d_{clu} = \frac{1}{2}$ between two clusters.

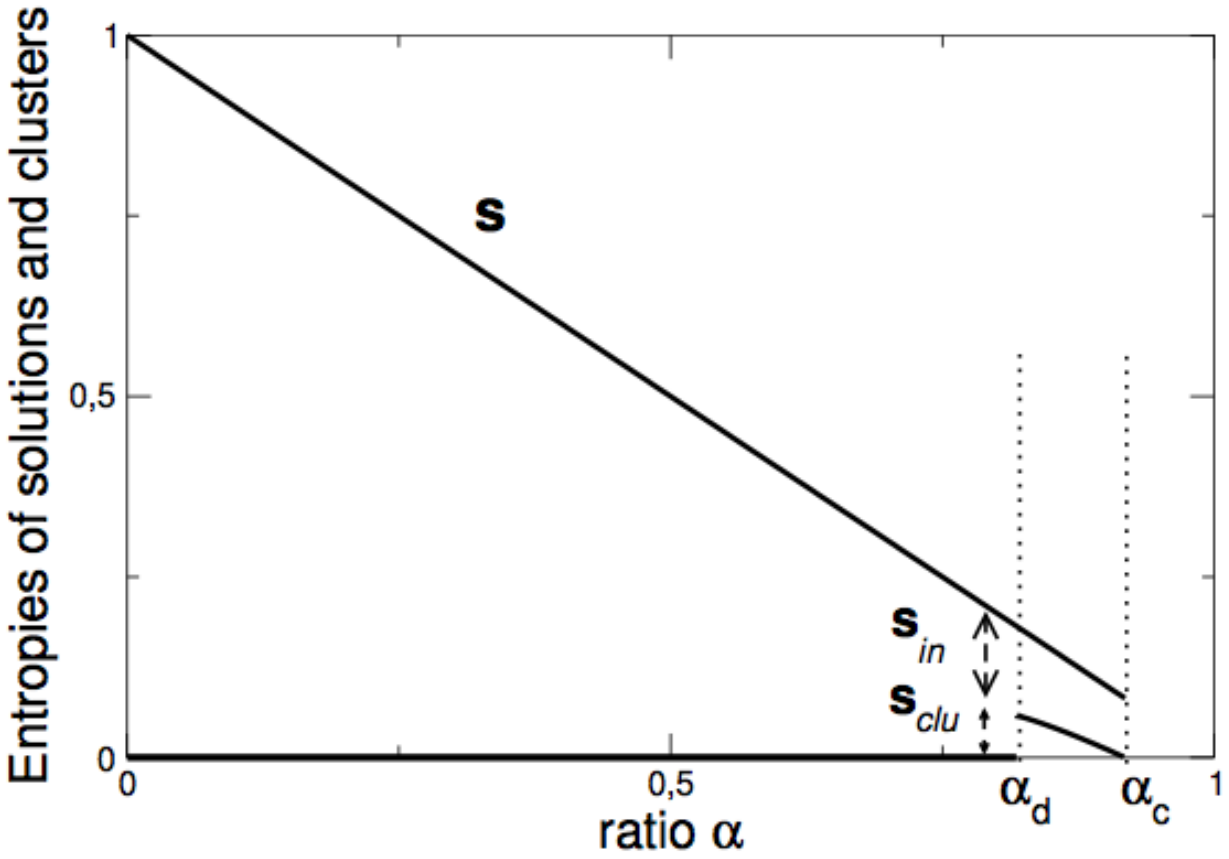


FIG. 2.3. Entropies (base 2 logarithms divided by size $N$) of the numbers of solutions and clusters as a function of the ratio $\alpha$. The entropy of solutions equals $1-\alpha$ for $\alpha < \alpha_c \simeq 0.918$. For $\alpha < \alpha_d \simeq 0.818$, solutions are uniformly scattered on the $N$-dimensional hypercube. At $\alpha_d$ the solution space discontinuously breaks into disjoint clusters. The entropies of clusters, $s_{cluster}$, and of solutions in each cluster, $s_{in}$, are such that $s_{cluster} + s_{in} = s$. At $\alpha_c$ the number of clusters stops being exponentially large ($s_{cluster} = 0$). Above $\alpha_c$ there is almost surely no solution.

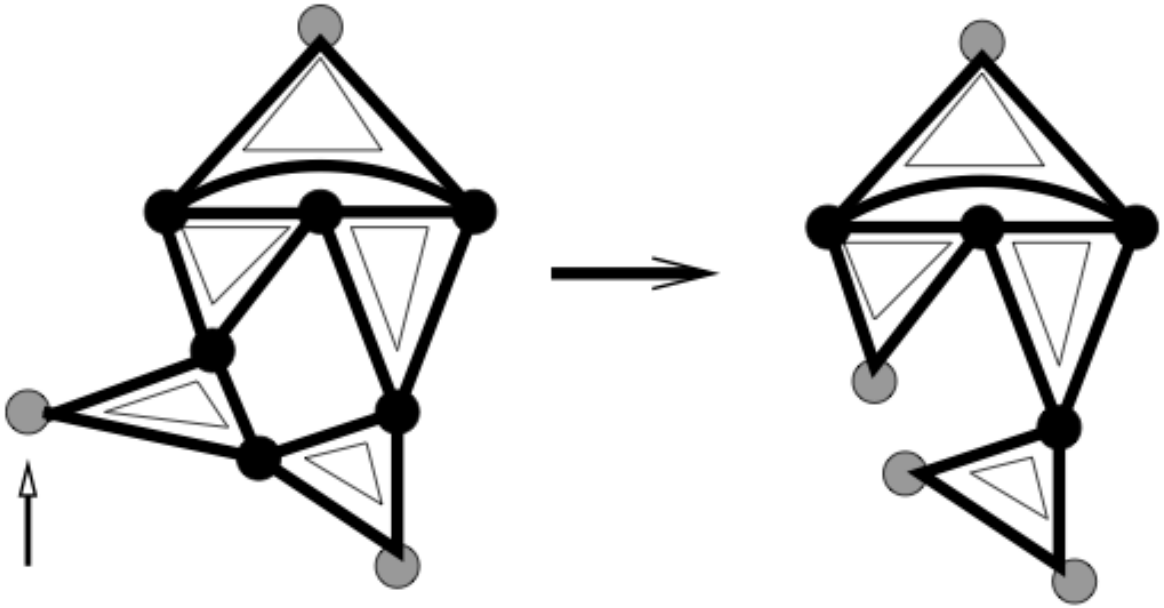

FIG. 2.2. Graph representation of the 3-XORSAT formula. Vertices (variables) are joined by plaquettes (values 0, 1 of second members are not shown here). A step of decimation consists in listing all 1-variables (appearing only once in the formula, shown by gray vertices), choosing randomly one of them (gray vertex pointed by the arrow), and eliminating this variable and its plaquette. New 1-variables may appear. Decimation is repeated until no 1-variable is left.

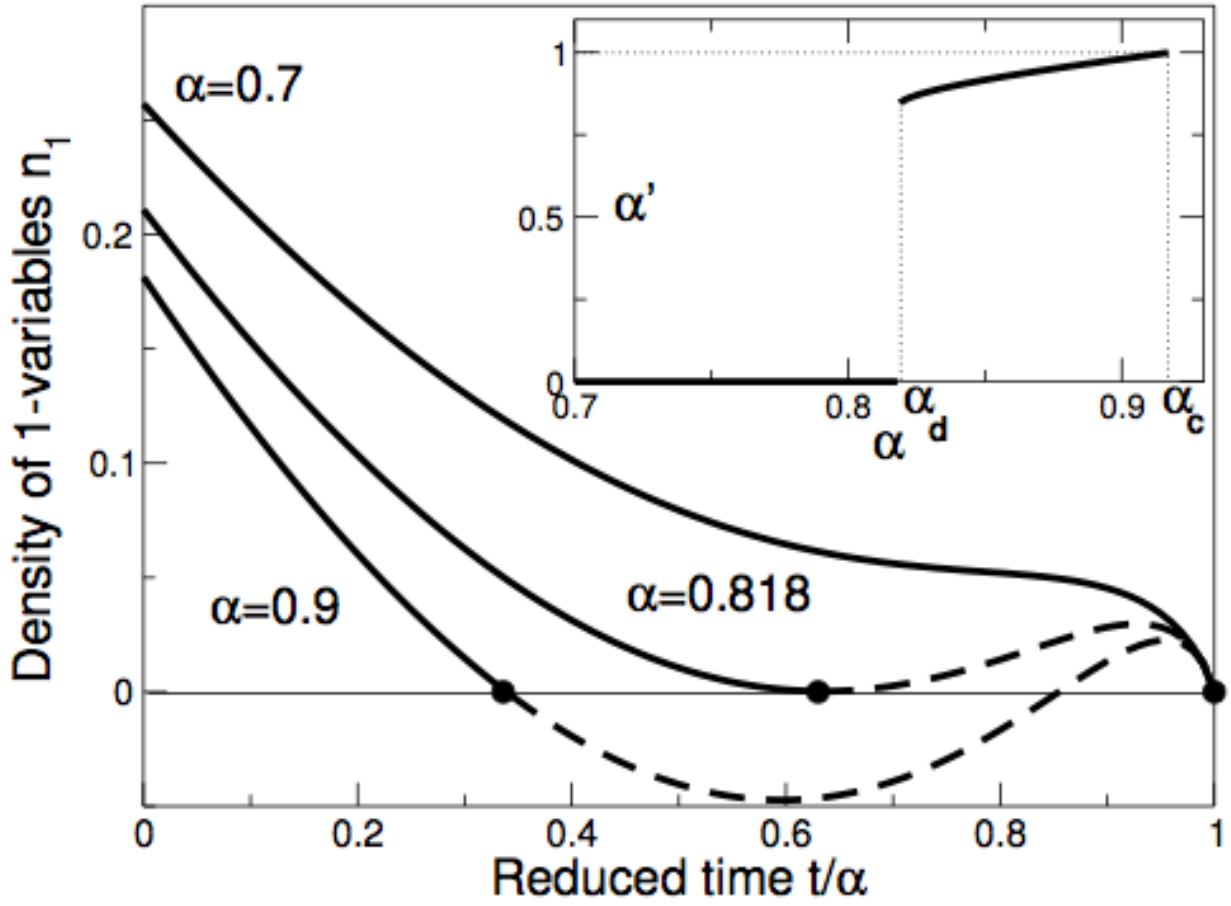


FIG. 2.5. Evolution of the density of 1-variables $n_1(t)$ generated by the decimation procedure. For $\alpha < \alpha_d \simeq 0.818$, $n_1(t)$ remains positive until all the plaquettes are eliminated at $t^* = \alpha$. For $\alpha > \alpha_d$ the decimation procedure stops at the time $t^*$ for which $n_1$ vanishes (black dots), and the solution of eqn. (2.7) is non physical for $t > t^*$ (dashed part of the curves). Notice that $t^*$ discontinuously jumps down at $\alpha = \alpha_d$ (first order transition). Inset: plaquette density $\alpha'$ for the reduced formula $F_2$ vs. $\alpha$. At $\alpha = \alpha_d$, $\alpha'$ discontinuously jumps to a positive value; the threshold $\alpha' = 1$ for the disappearance of solution is reached for $\alpha_s \simeq 0.918$.

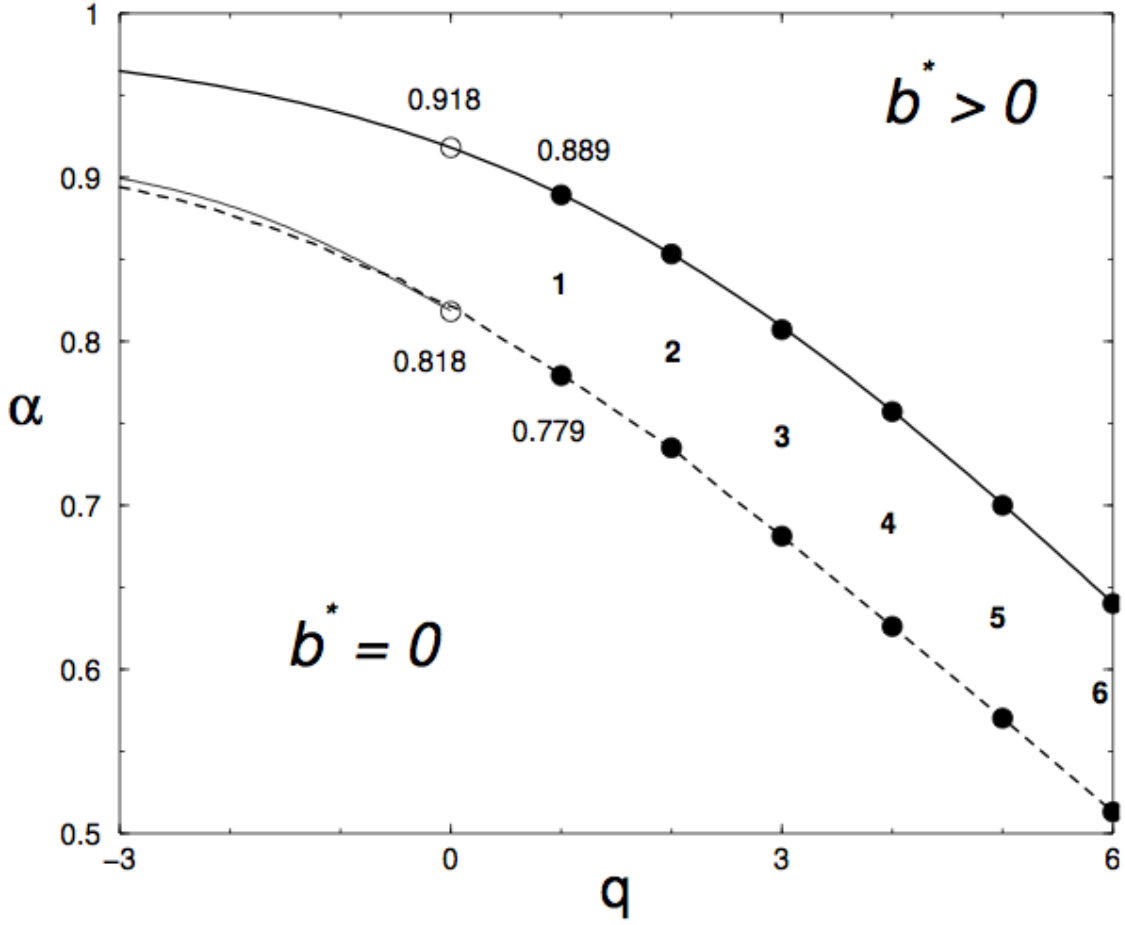


FIG. 2.6. The $q, \alpha$ plane and the critical lines $\alpha_M(q)$ (dashed), $\alpha^*(q)$ (full tick), and $\alpha_s(q)$ (full thin) appearing in the calculation of the $q^{th}$ moment for homogeneous 3-XORSAT systems. Full dots correspond to integer $q$ values, while continuous curves result from the analytic continuation to real $q$. The fraction of variables in the backbone, $b^*$, vanishes below the line $\alpha_M(q)$; the global maximum of $A_h$ in (2.31) is located in $b^* > 0$ for ratios $\alpha > \alpha^*(q)$. Ansatz (2.29) is locally unstable in the hardly visible domain $q < 0, \alpha_M(q) < \alpha < \alpha_s(q)$.

## Exercise:

Let us consider the following heuristic algorithm to solve 3-XORSAT formulae, called Unit-Clause (UC) procedure. Initially all variables are unassigned. At time t=0, if there is no clause (equation) with a single variable, a variable is randomly picked up and set to 1 or 0 with probability $\frac{1}{2}$. If there is one equation with a single variable, e.g. $x_1 = 1$, then its variable is assigned to satisfy the clause; in case of more than one equation with a single variable one such equation is picked up uniformly at random. The algorithm stops when all equations have disappeared (are satisfied), or when a contradiction is found (two opposite equations $x_i = 0$ and $x_i = 1$ are found). Calculate the probability that this algorithm solves successfully a random 3-XORSAT formula as a function of the ratio $\alpha$ in the infinite $N$ limit.

**Monday:**

Random graphs: typical & rare properties of structure
(nb, size, nature of components, cycles, …)

**Tuesday**

Interacting models on random graphs (phase transitions)
with 2 approaches:

- Modeling of dynamical changes of a graph (cf. N. Wormald's paper)
- Replica method (spin glasses, RMT, …)

**Today**

Random spatial maps and spin glass models

**Multidimensional scaling in statistics:**

Set of towns i=1,…,N
Distance matrix $d_{ij}$

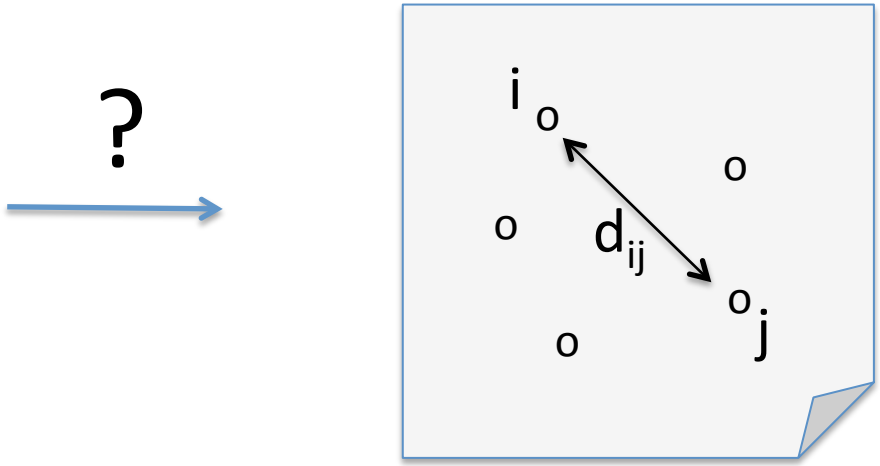

## Multidimensional scaling in statistics:

- Extension to 'qualitative' measures of distances (non classical scaling)
- Many applications in social sciences, biology, …
- Connections with: Dimensional reduction (PCA), Network inference (Hopfield model)
- Here, more abstract: 2 spaces

# Storage of spatial maps in an attractor neural network model of the hippocampus

Netadis Summer School on Complex Systems, Hillerod, September 2013

# Plan

- Biological facts and motivations
- Model and statistical mechanics framework
- Storage of environments (spatial charts)
- Dynamics within one chart
- Transitions between charts
- Conclusion & Perspectives

# Representation of Space in the Brain

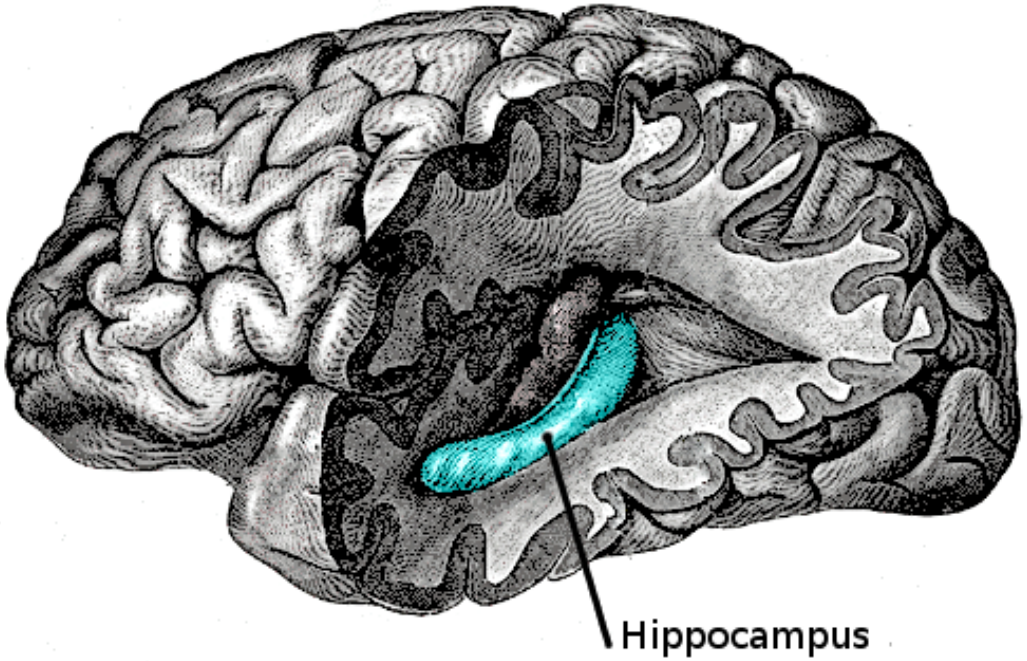


Electrode recordings: O'Keefe & Dostrovsky (1971)
Cells in the Hippocampus respond to position in space in a specific way (called place cells)

# Place cells

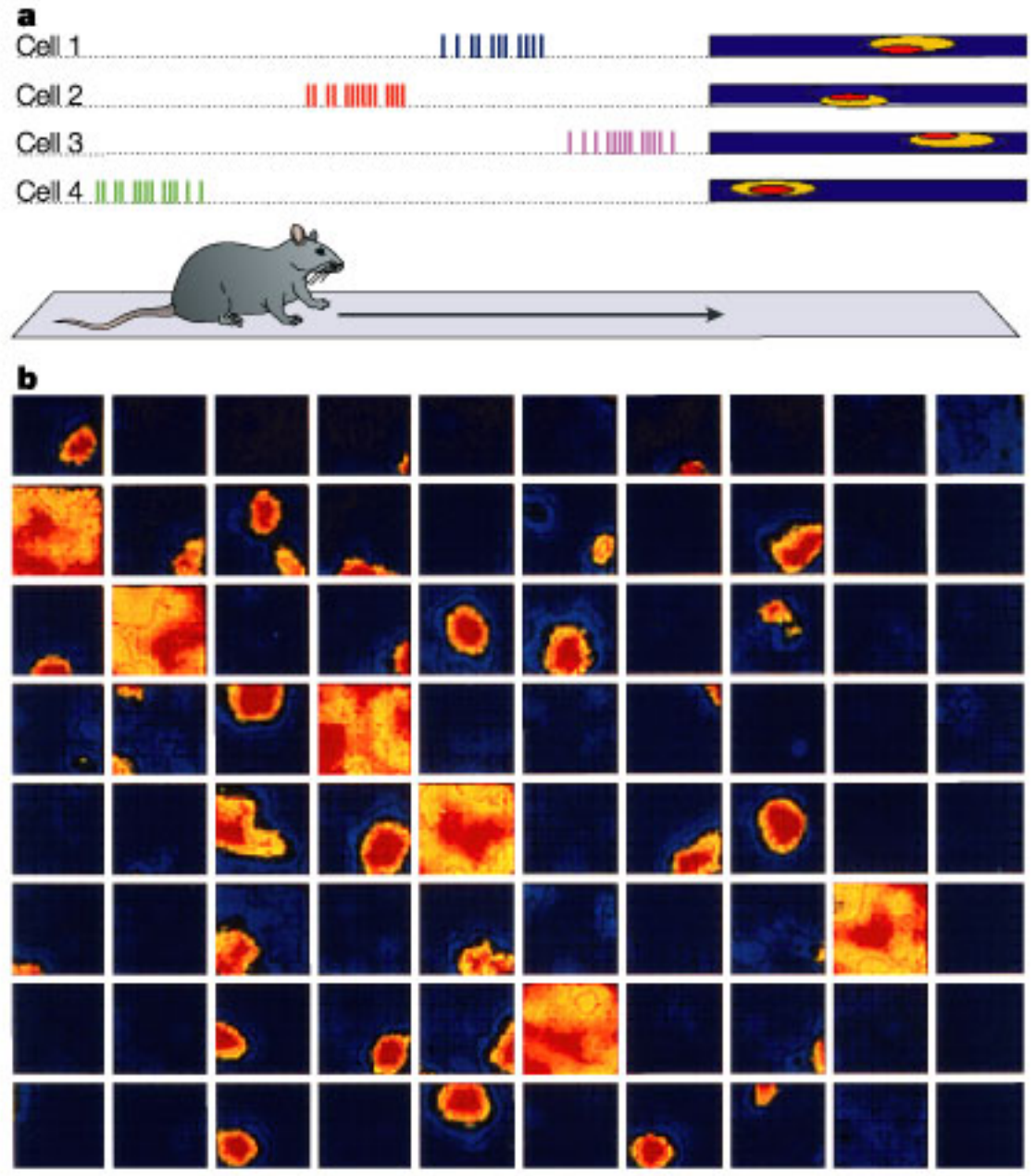


Kazu Nakazawa, Thomas J. McHugh, Matthew A. Wilson & Susumu Tonegawa
*Nature Reviews Neuroscience* **5**, 361-372 (May 2004)

# Where do place fields come from?

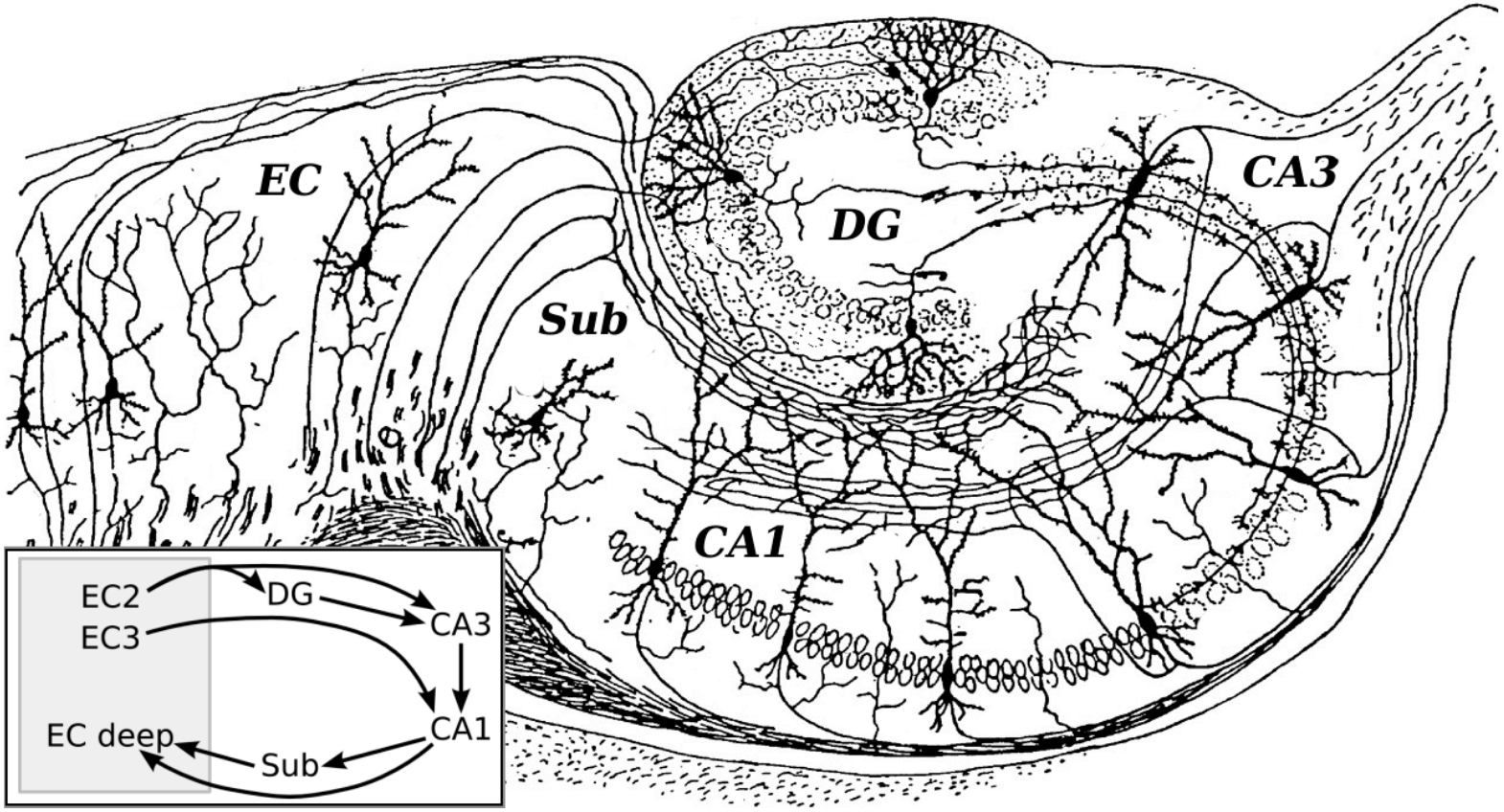


Medio-enthorinal cortex ➔ Hippocampus

# Grid cells

Hafting, Fyhn, Molden, Moser & Moser, Nature 436, 801-806 (2005)

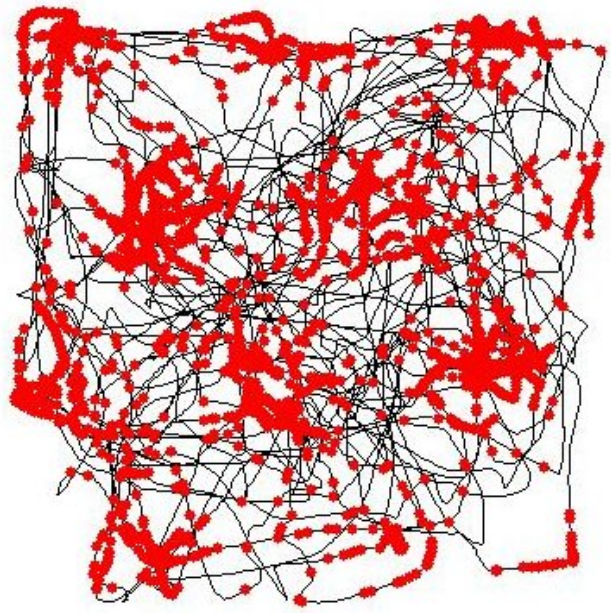

*Trajectory of a rat through a square environment is shown in black. Red dots indicate locations at which a particular entorhinal grid cell fired.*

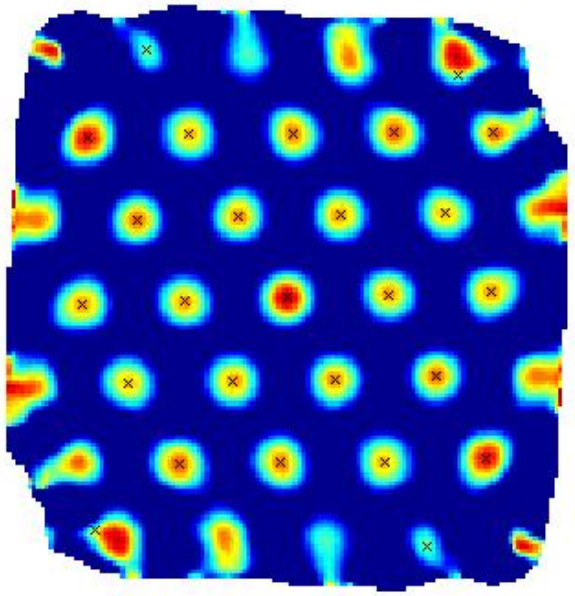

*Spatial autocorrelogram of the neuronal activity of the grid cell from the left figure.*

- weighted sums of grid cell activities may produce localized activity (place fields)
- changes in weights results in 'random' remappings

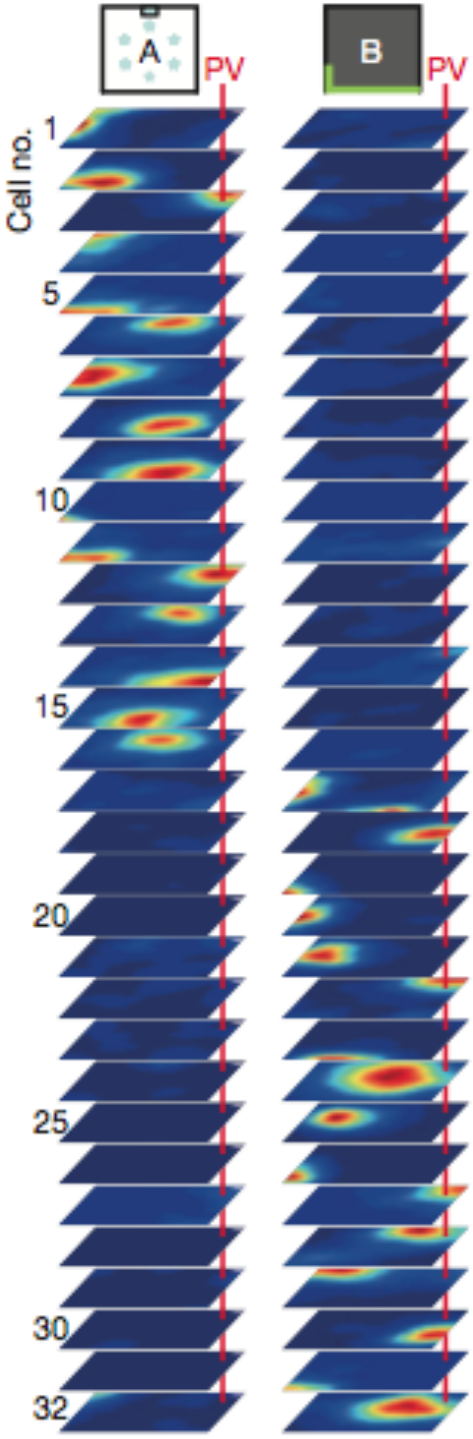


# Teleportation (1)

- Rat in 2 different environments
- Place fields are specific to each environment
- Population vectors (average activity) specific to each environment
- Sudden changes of environment?

Jezek, Henriksen, Treves, Moser & Moser, Nature 478, 246 (2011)

# Teleportation (2)

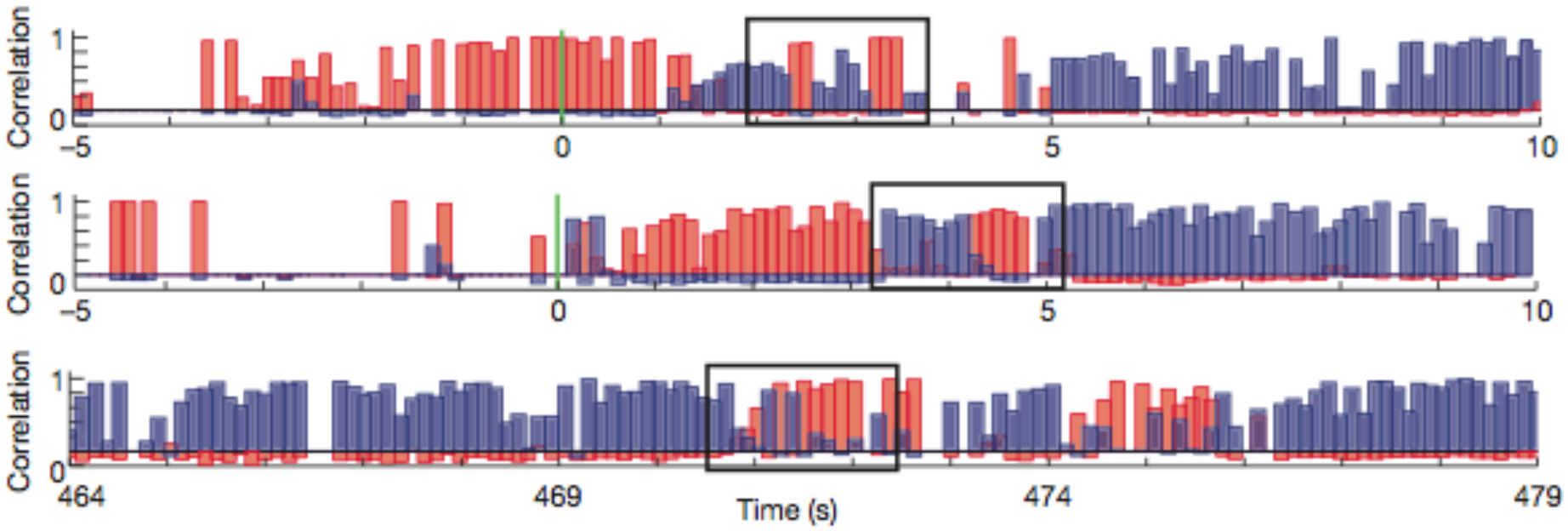


How are different environments ‘stored’ in the hippocampus?
What is the dynamics of the neural activity within one environment?
In between two environments?

# Model: one environment (1)

Neuron = binary state, silent or active : $\sigma_i = 0,1$

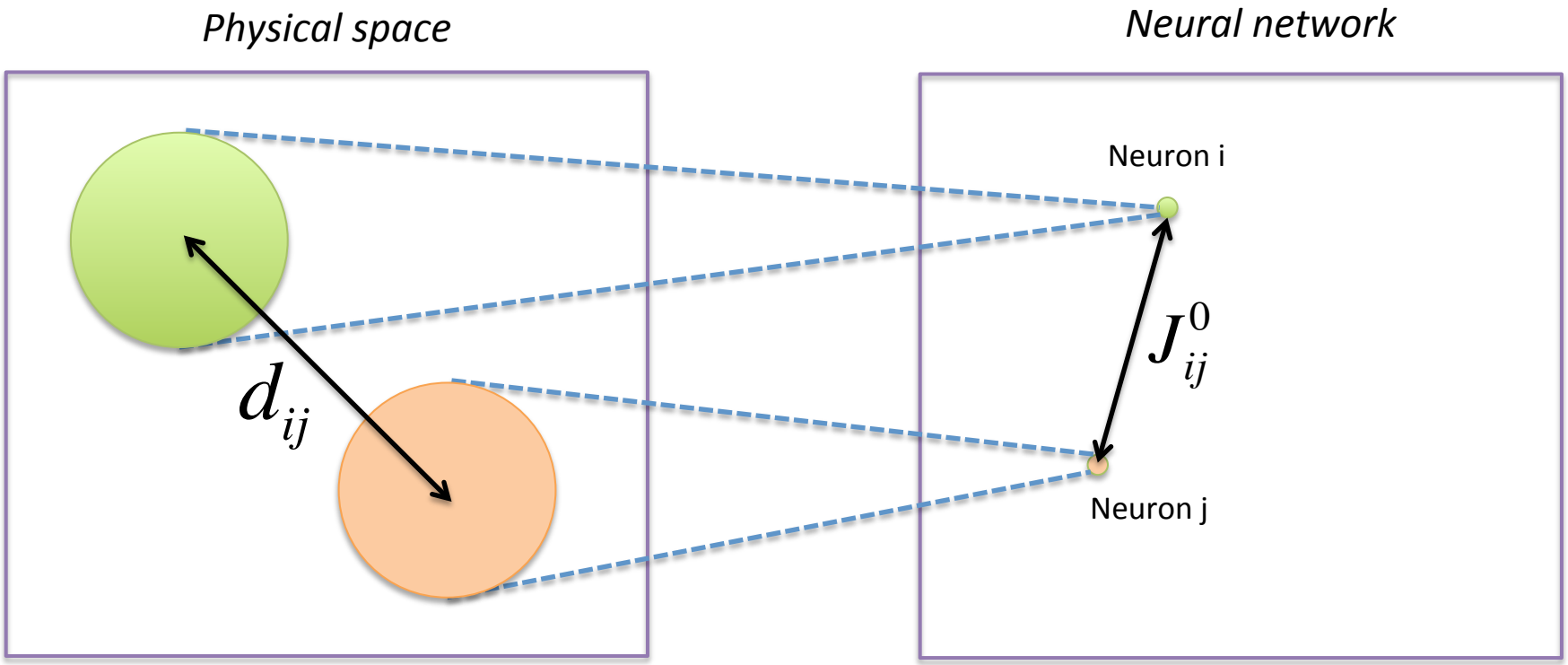


$$J_{ij}^0 = \begin{cases} \frac{1}{N} & \text{if } d_{ij} \leq d_c \ , \\ 0 & \text{if } d_{ij} > d_c \end{cases}$$

# Model: one environment (2)

*Physical space*

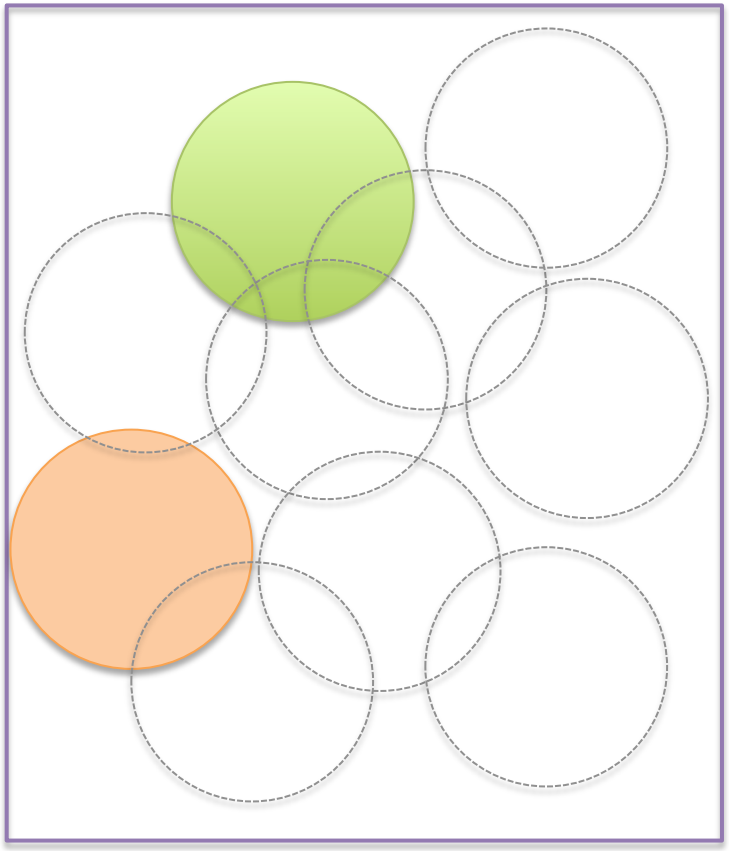

*Neural network*

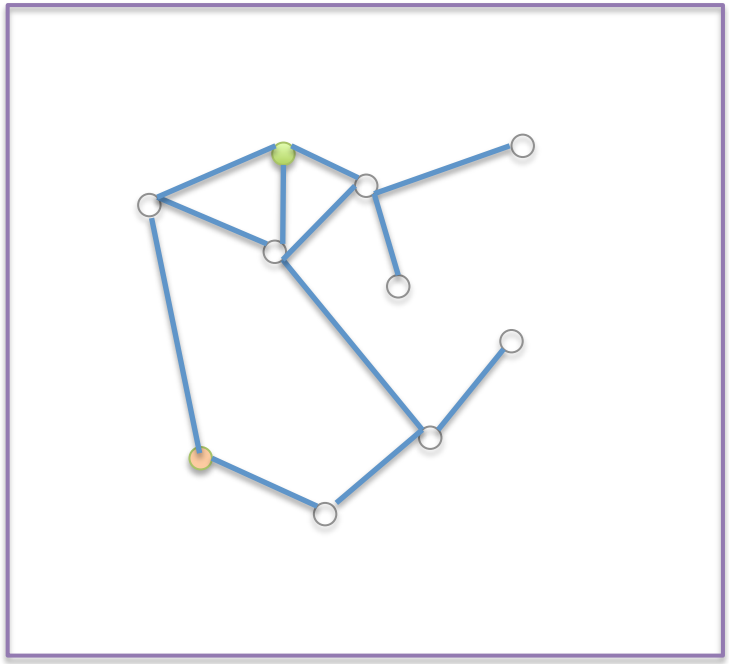

$$J_{ij}^0 = \begin{cases} \frac{1}{N} & \text{if } d_{ij} \leq d_c \\ 0 & \text{if } d_{ij} > d_c \end{cases},$$

- we choose $d_c$ so that each neuron is connected to $wN$ other neurons ($w$<<1, but long range interactions)
- Interaction matrix invariant under translations (not necessary)

# Model: random remappings

Hypothesis: place fields are randomly remapped onto neurons

Example in dimension D=1:

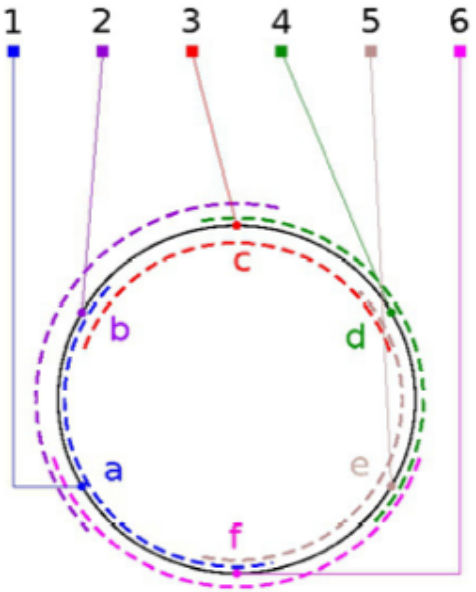


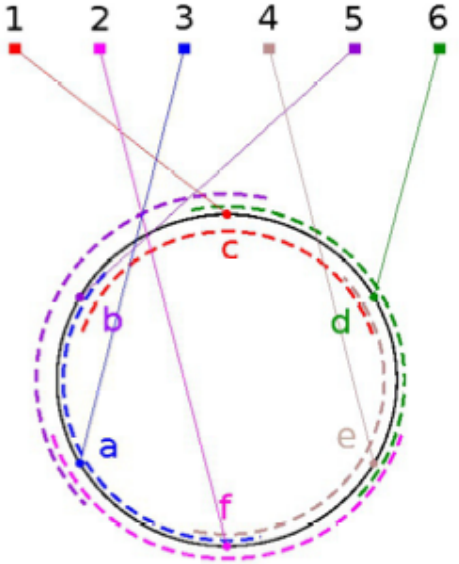


New environment = random permutation π

Battaglia, Treves (1998);
Tsodyks (1999); Hopfield (2010)

# Model: statistical mechanics formulation

Interaction matrix for L+1 environments:

$$J_{ij} = \sum_{\ell=0}^{L} J_{ij}^{\ell} = J_{ij}^{0} + \sum_{\ell=1}^{L} J_{\pi^{\ell}(i)\pi^{\ell}(j)}^{0}$$

Probability of activity configuration:

$$P_J(\boldsymbol{\sigma}) = \frac{1}{Z_J(T)} \exp\left(-E_J[\boldsymbol{\sigma}]/T\right)$$

'Energy' : (=-log likelihood)

$$E_J[\boldsymbol{\sigma}] = -\sum_{i<j} J_{ij}\,\sigma_i\,\sigma_j$$

Partition function:

$$Z_J(T) = \sum_{\boldsymbol{\sigma} \text{ with constraint } \sum_{i=1}^{N} \sigma_i = f\,N} \exp\left(-E_J[\boldsymbol{\sigma}]/T\right)$$

(inhibition)

# Case of a single environment (1)

Translation-invariant and long-range interactions: exactly solvable model
(J.L. Lebowitz and O. Penrose, Journal of Mathematical Physics 7, 98 (1966))

Order parameter =
Coarse-grained activity:

$$\rho(x) \equiv \lim_{\epsilon \to 0} \lim_{N \to \infty} \frac{1}{\epsilon N} \sum_{(x-\frac{\epsilon}{2})N \leq i < (x+\frac{\epsilon}{2})N} \langle \sigma_i \rangle_J$$

Single neuron
self-consistent
equations:

$$\rho(x) = \frac{1}{1 + e^{-\mu(x)/T}} ,$$

$$\mu(x) = \int \mathrm{d}y \, J_w(x-y)\rho(y) + \lambda$$

(imposes global activity)

(Similar to rate model for neurons)

# Case of a single environment (2)

T=0

*Localized phase*

$T_{spinodal}$

*Paramagnetic phase*

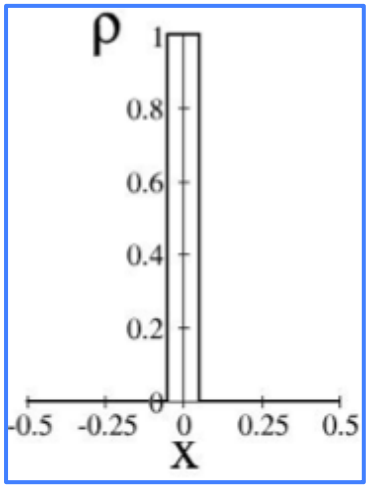


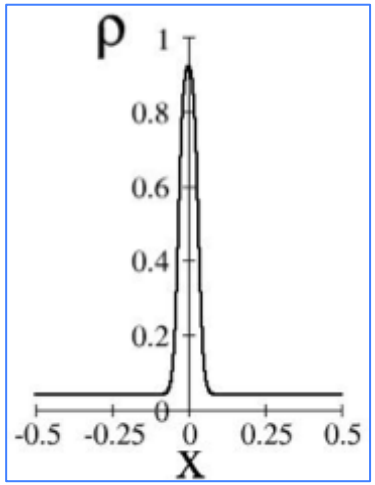


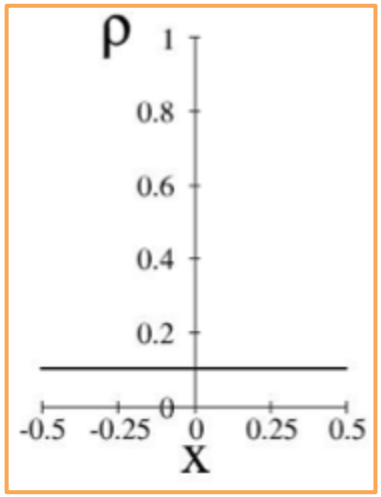


True also in D=2:

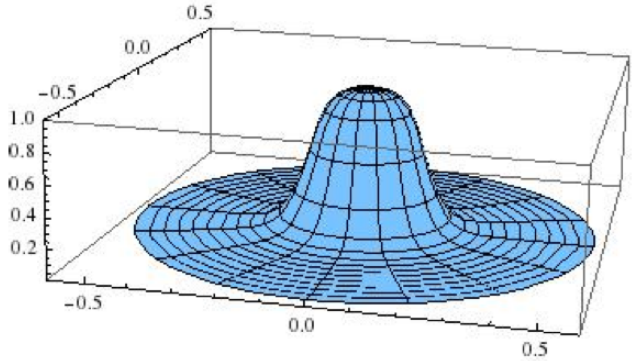

# Multi-environment case: averaging over remappings

Free energy depends on realization of random interactions J
= permutations $\pi_1, \pi_2, \ldots, \pi_L$

Hypothesis: concentration when N➔∞

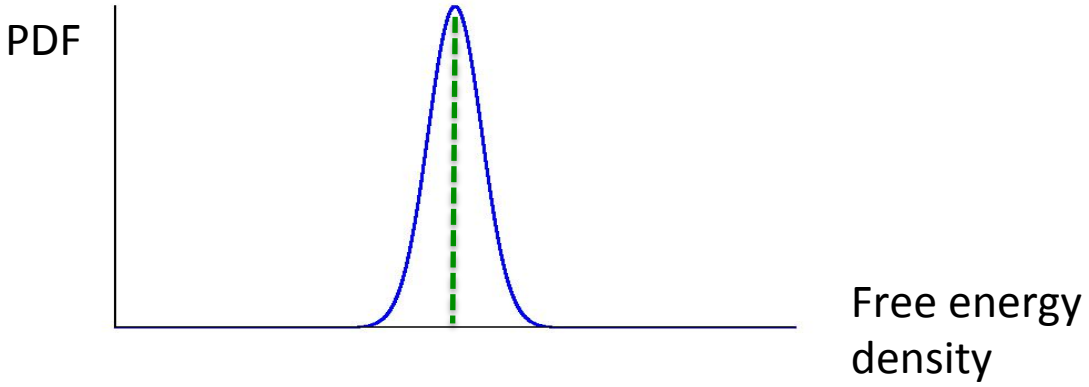


Replica method: $$\overline{Z_J(T)^n} = \int df \mu_N(f) e^{N(-n\beta f)} = e^{N(-n\beta f_{av} + \frac{n^2}{2}\Gamma + O(n^3)) + o(N)}$$

Average free energy

Fluctuations

# Multi-environment case: averaging over remappings

$$\overline{Z_J(T)^n} = \overline{\sum_{\vec{\sigma}} \exp\left[\beta \sum_{a=1}^{n} \sum_{i<j} \left( J_{ij}^0 + \sum_{\ell=1}^{L} J_{ij}^{\ell} \right) \sigma_i^a \sigma_j^a \right]}$$

$$= \sum_{\vec{\sigma}} \exp\left[\beta \sum_{a=1}^{n} \sum_{i<j} J_{ij}^0 \, \sigma_i^a \sigma_j^a \right] \Xi(\vec{\sigma})^L \,, \quad \text{where}$$

$$\Xi(\vec{\sigma}) = \frac{1}{N!} \sum_{\pi^\ell} \exp\left[\beta \sum_{i<j} J_{ij}^0 \sum_{a=1}^{n} \sigma_{\pi^\ell(i)}^a \sigma_{\pi^\ell(j)}^a \right]$$

Average over permutations is not immediate … but can be done when N➔∞
(some similarity with Itzykson-Zuber integral, but discrete group here)

$$\log \Xi(\vec{\sigma}) = -\frac{\beta}{2} n f(1-f) + N \frac{\beta}{2} n w f^2$$

$$- \sum_{\lambda \neq 0} \text{Trace } \log\left[\mathbf{Id}_n - \beta\lambda(\mathbf{q} - f^2 \, \mathbf{1}_n)\right]$$

$$q^{ab} \equiv \frac{1}{N} \sum_j \sigma_j^a \sigma_j^b$$

# Multi-environment case: order parameters

Local density of activity averaged over environments:

$$\rho(x) \equiv \lim_{\epsilon \to 0} \lim_{N \to \infty} \frac{1}{\epsilon N} \sum_{(x-\frac{\epsilon}{2})N \leq i < (x+\frac{\epsilon}{2})N} \overline{\langle \sigma_i \rangle_J}$$

Edwards-Anderson overlap (measures spatial heterogeneities in the activity):

$$q \equiv \frac{1}{N} \sum_{i=1}^{N} \overline{\langle \sigma_i \rangle_J^2}$$

# Phases and Transition Lines

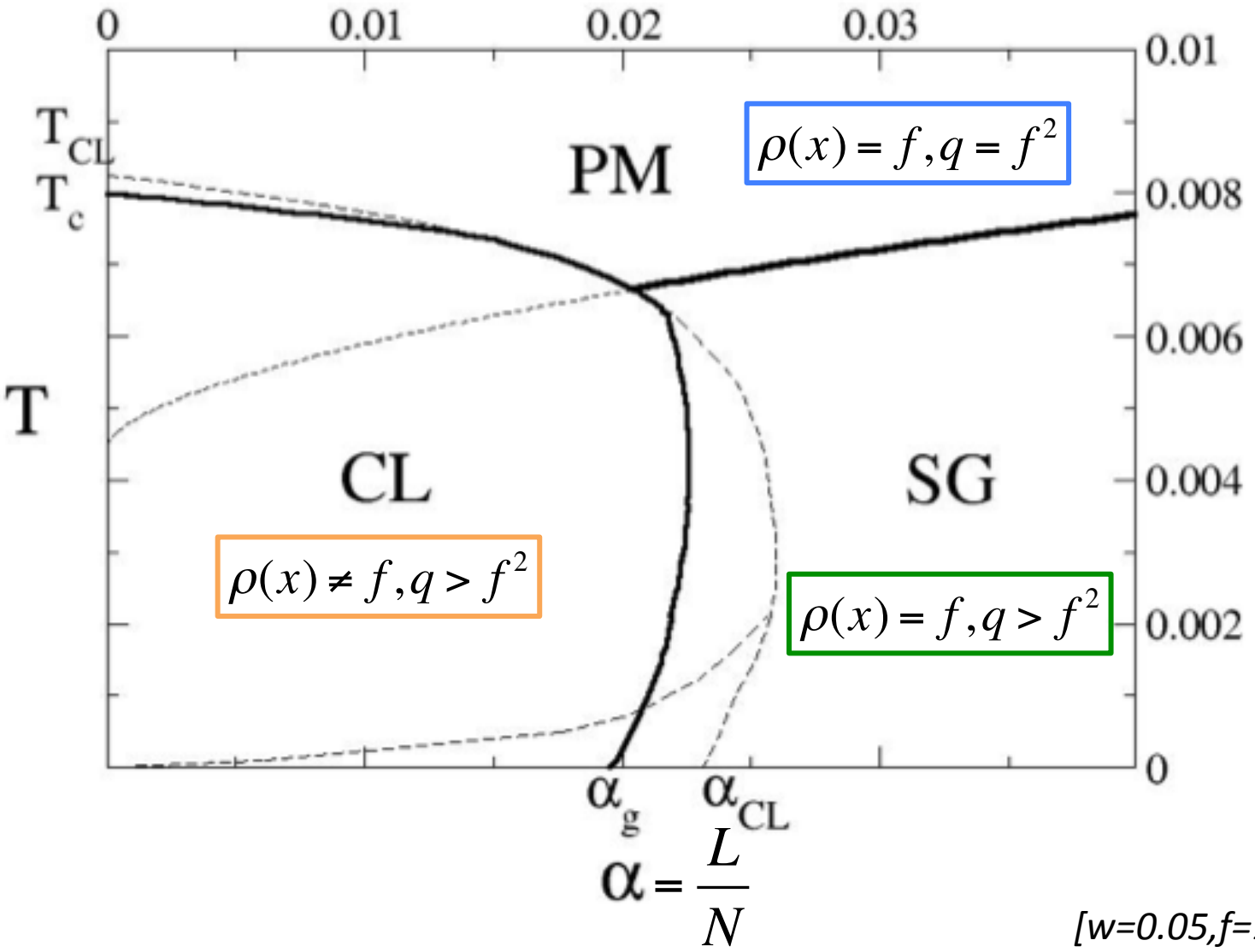


*[w=0.05,f=1,D=1]*

# Simulations and Dynamics

Monte Carlo Dynamics:

- Pick up one silent (index i) and one active spin (index j)
- Compute variation of energy when spins are swapped

$$\Delta E = -\sum_{k(\neq i,j)} \left(J_{ik} - J_{jk}\right)\sigma_k$$

- Accept according to detailed balance, e.g. Metropolis

$$\frac{\omega(\Delta E)}{\omega(-\Delta E)} = \exp(-\beta\,\Delta E)$$

# Simulations and Dynamics

Observe:

- Static properties …
- Stability and fluctuations of clump (=quasi-particle?)
- Motion of clump within one environment
- Transitions between environments

# Check of equilibrium properties

Local field acting on spin i:

$$h_i = \sum_j J_{ij}^0 \sigma_j + \sum_{l,j} J_{ij}^l \sigma_j$$

μ(x)

Gaussian random variable of variance α r, (r = conjugated parameter to q)

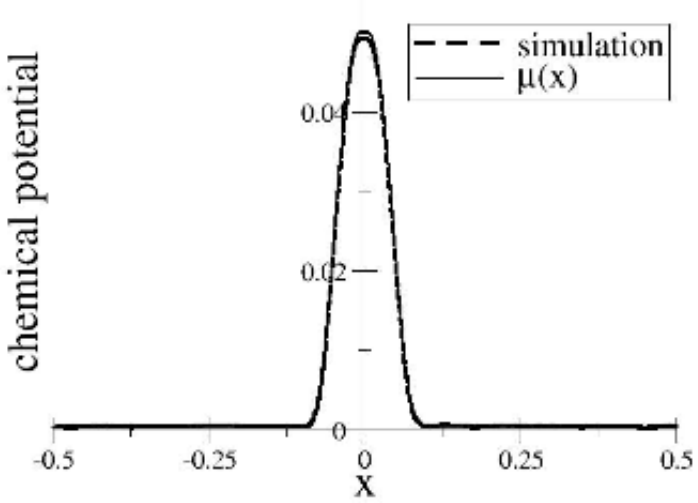


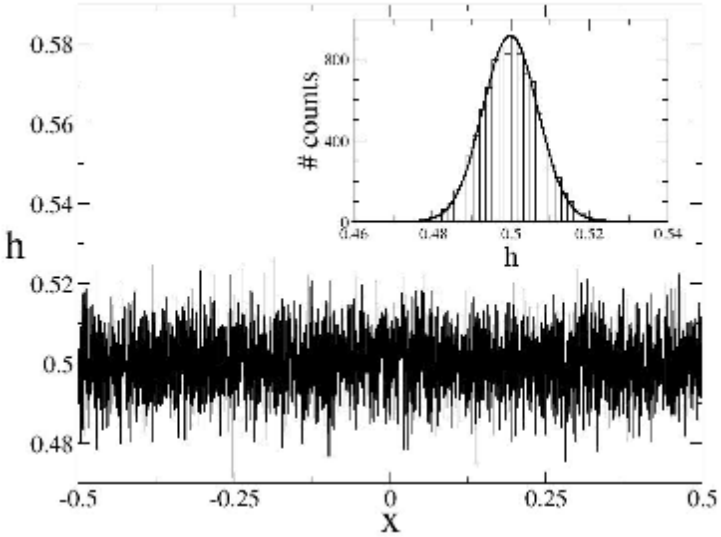


*(D=1, N=10000, T=0.004, α=0.01)*

# Dynamics within one environment (1)

Trajectory of clump center in D=2
(N=45x45 spins, α=0.001, T=0.004)

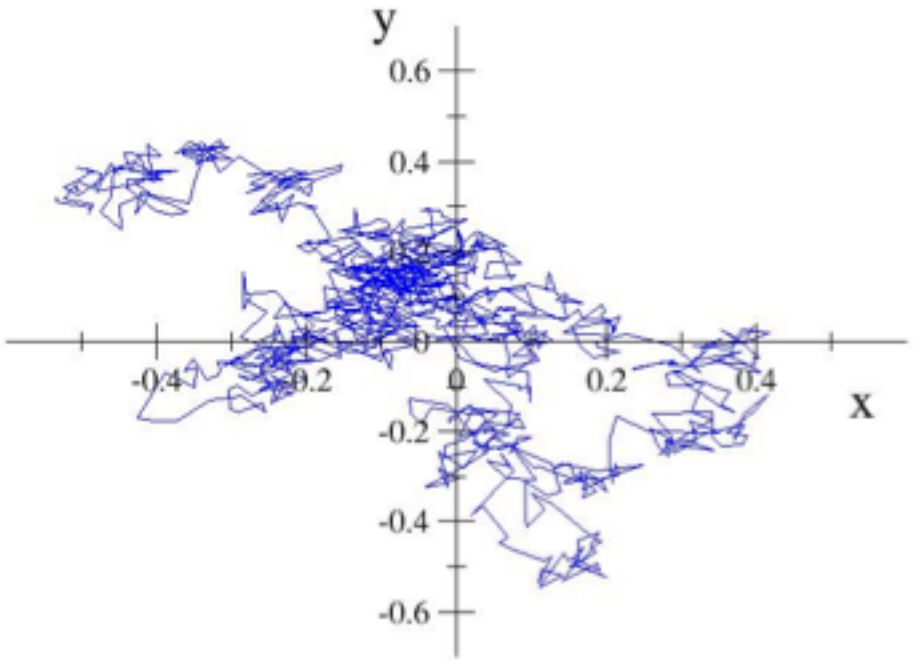


Position of clump center in D=1 as a function of time (MC rounds= t x 20)
(N=2000 spins, α=0.003, T=0.006)

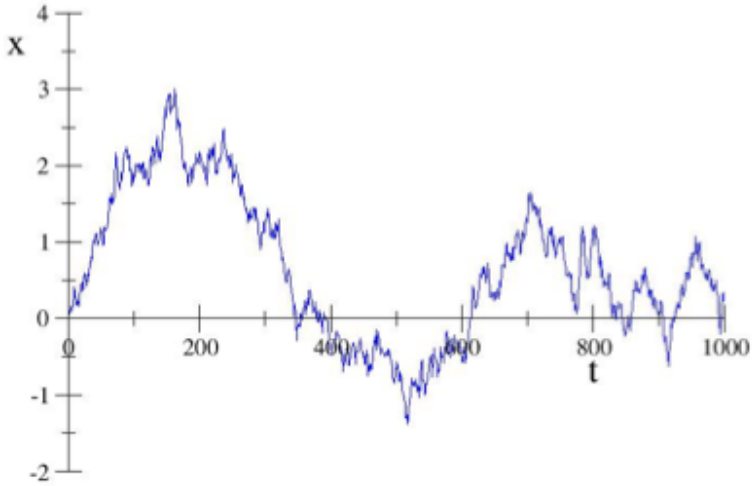

# From spin configuration dynamics to density dynamics (1)

**Flip spins i=Na and j=Nb:**

**(0 to 1) (1 to 0)**

$$\Delta\rho(x) = \frac{1}{N}\delta(x-a) - \frac{1}{N}\delta(x-b)$$

**Change in free energy:**

$$\begin{aligned}
\Delta\mathcal{F} &= N\,\mathcal{F}[\boldsymbol{\rho}+\Delta\boldsymbol{\rho}] - N\,\mathcal{F}[\boldsymbol{\rho}] \\
&= \frac{\delta\mathcal{F}}{\delta\rho(a)} - \frac{\delta\mathcal{F}}{\delta\rho(b)} \\
&= -\int dx\,\big(J_w(a-x) - J_w(b-x)\big)\,\rho(x) \\
&\quad + T\log\left[\frac{\rho(a)}{(1-\rho(a)}\right] - T\log\left[\frac{\rho(b)}{(1-\rho(b)}\right]
\end{aligned}$$

# From spin configuration dynamics to density dynamics (2)

**Rate of flip:**

$$\begin{aligned}\hat{\omega}(\boldsymbol{\rho}; a, b) &= (1-\rho(a))\rho(b)\,\omega(\Delta E) \\ &= N(1-\rho(a))\rho(b)\times \\ &\quad \omega\left(-\int dx\,\left(J_w(a-x)-J_w(b-x)\right)\rho(x)\right)\end{aligned}$$

**Detailed balance:**

$$\frac{\hat{\omega}(\boldsymbol{\rho}; a, b)}{\hat{\omega}(\boldsymbol{\rho}+\Delta\boldsymbol{\rho}; b, a)} = \exp(-\beta\,\Delta\mathcal{F}[\boldsymbol{\rho}])$$

Hence, convergence towards equilibrium in the density profile space …

$$\rho(x) \;\rightarrow\; \rho^{*}(x) + \Delta\rho(x)$$

# The clump is a quasi-particle …

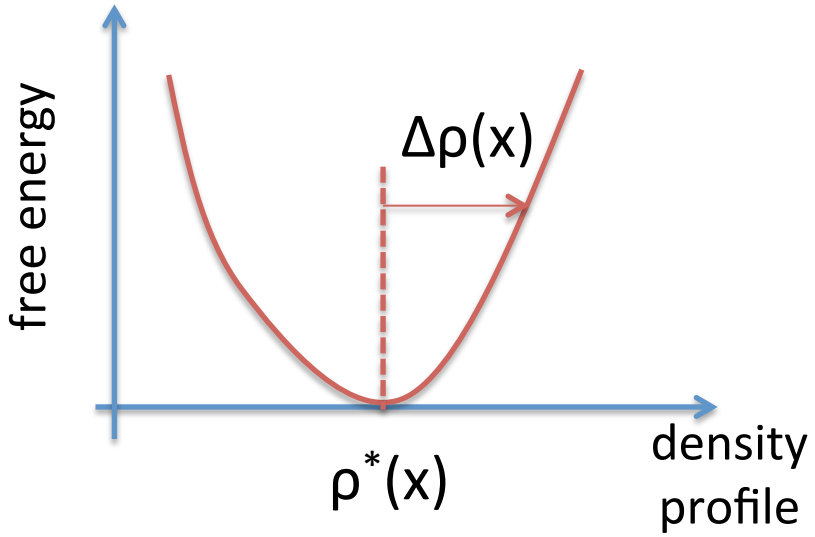


**Diffusion tensor**

$$D(x,y) = \langle \Delta\rho(x)\, \Delta\rho(y) \rangle$$

**Stiffness tensor**

$$H(x,y) = \left. \frac{\delta^2 \beta \mathcal{F}}{\delta\rho(x)\delta\rho(y)} \right|_{\rho^*}$$

➔ Relaxation towards equilibrium density for all modes, with thermalization at 'temperature' of the order of $N^{-1}$ except for zero mode (translation of clump), which diffuses with

$$D_0 = \frac{\int dx\, dy\, (1-\rho^*(x))\rho^*(y)\,\omega^*(x,y) \left( \frac{d\rho^*}{dx}(x) - \frac{d\rho^*}{dx}(y) \right)^2}{N \int dx\, \frac{d\rho^*}{dx}(x)^2}$$

where $\omega^*(x,y) \equiv \omega\left( -\int dz \left( J_w(x-z) - J_w(y-z) \right) \rho^*(z) \right)$

# …with weak fluctuations across environment

Calculation of $\delta\sigma_i^2 = \overline{(<\sigma_i> - \overline{<\sigma_i>})^2} = q(x) - \rho^2(x)$

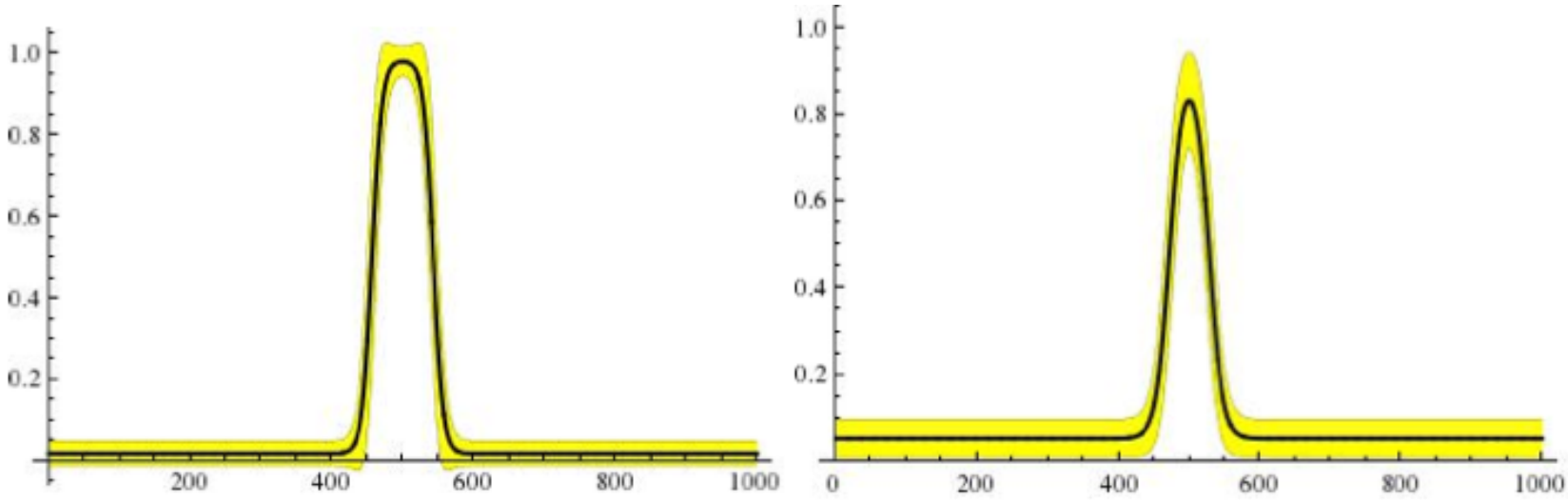


*(D=1, f=0.1, w=0.05, left: T=0.005, right: T=0.007)*

# Dynamics within one environment (2)

$$\overline{Z_J(T)^n} = \int df \mu_N(f) e^{N(-n\beta f)} = e^{N(-n\beta f_{av} + \frac{n^2}{2}\Gamma + O(n^3)) + o(N)}$$

Fluctuations

$$(\overline{\Delta F^2})^{1/2} = T\sqrt{\Gamma}\sqrt{N}$$

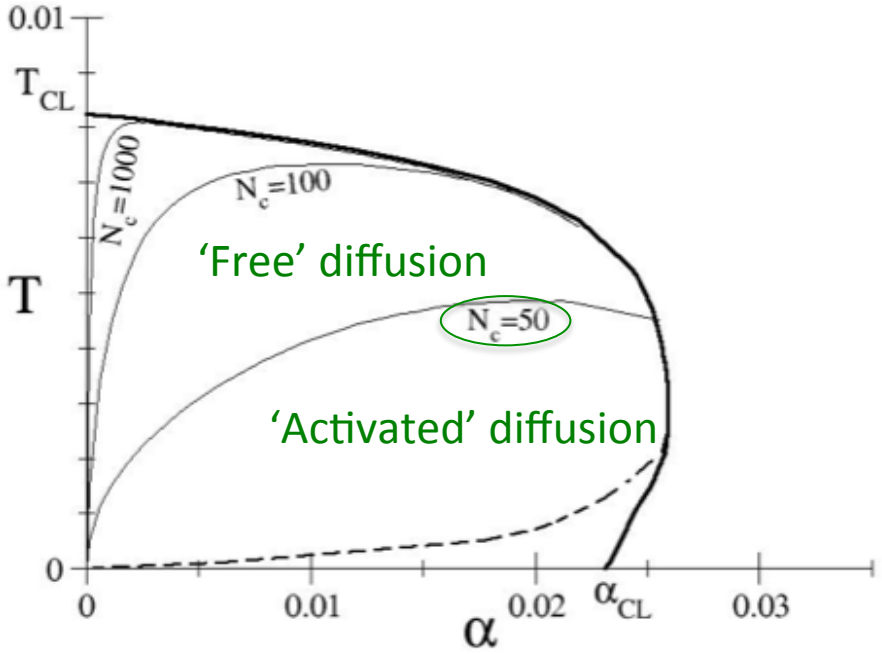


We can go further …

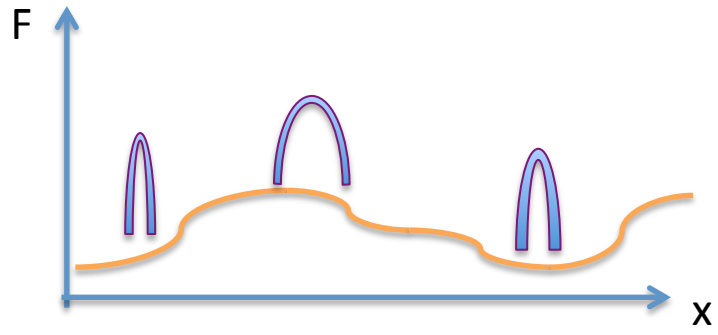


Compute $(\overline{\Delta F(x)\Delta F(y)})^{1/2} = T\sqrt{\Gamma(x-y)}\sqrt{N}$

Technically: two sets of n/2 replicas, n➔0

# Dynamics within one environment (3)

We expect $d \approx \frac{1}{N} e^{-\sqrt{N} G(\alpha,T)}$

Diffusion coefficient (log. scale)

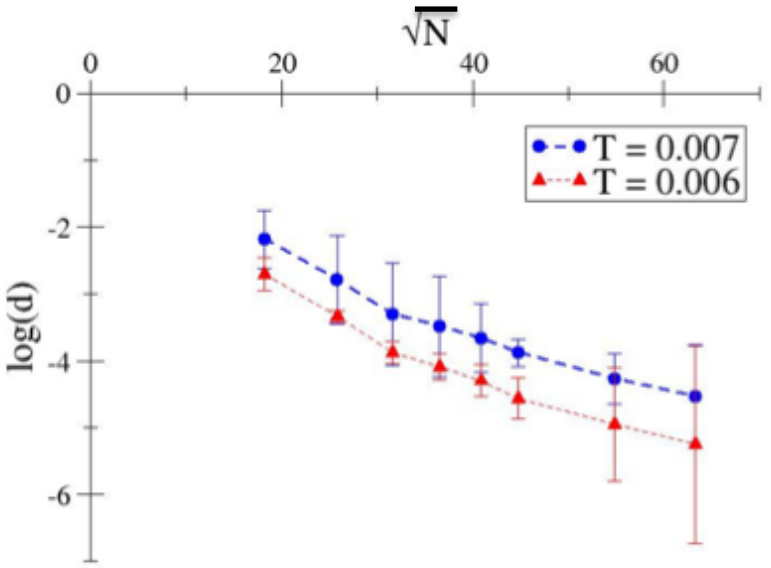


*[D=1,*
*N=1000,*
*T=0.006,*
*α=0.003,*
*10000 rounds]*

Chart-to-chart fluctuations

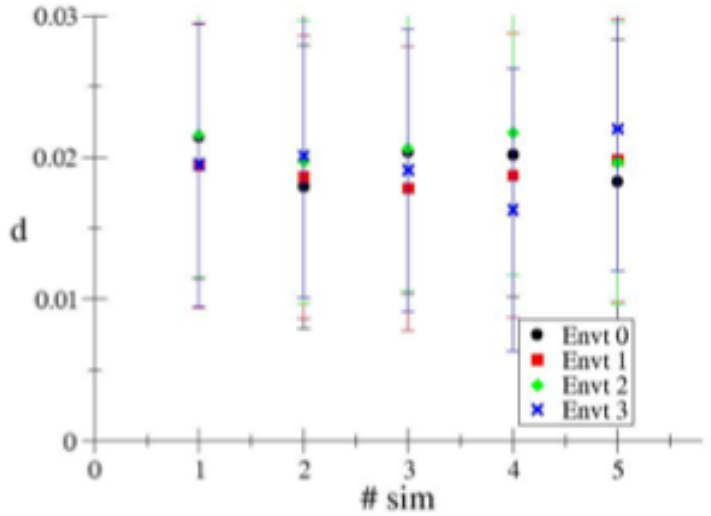

# Dynamics: transitions between environments

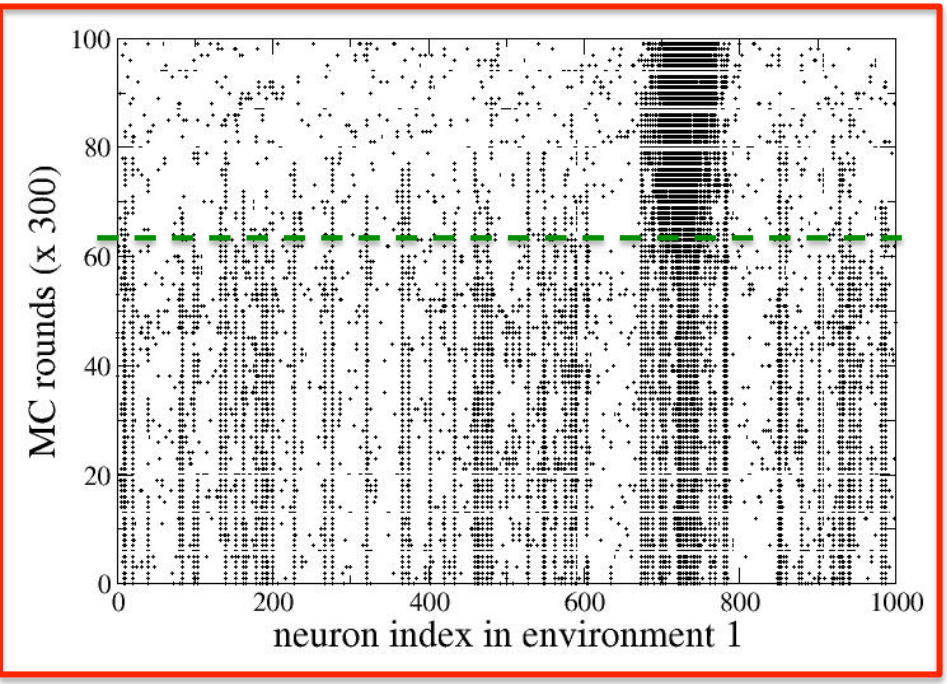


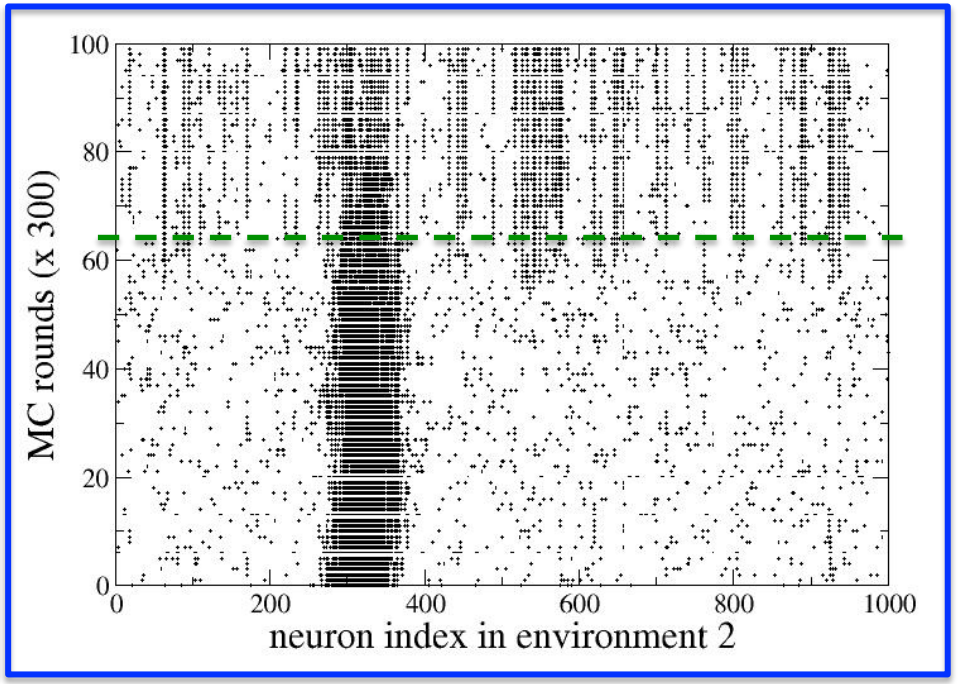


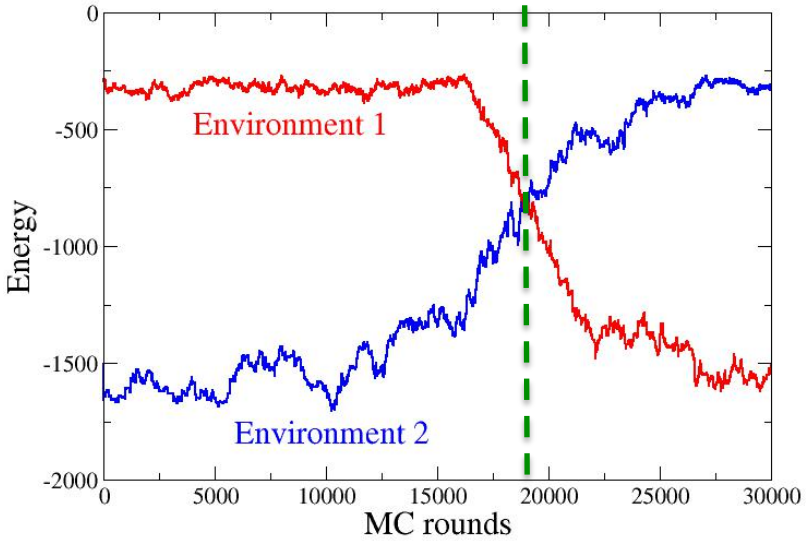

# Dynamics: transitions between environments

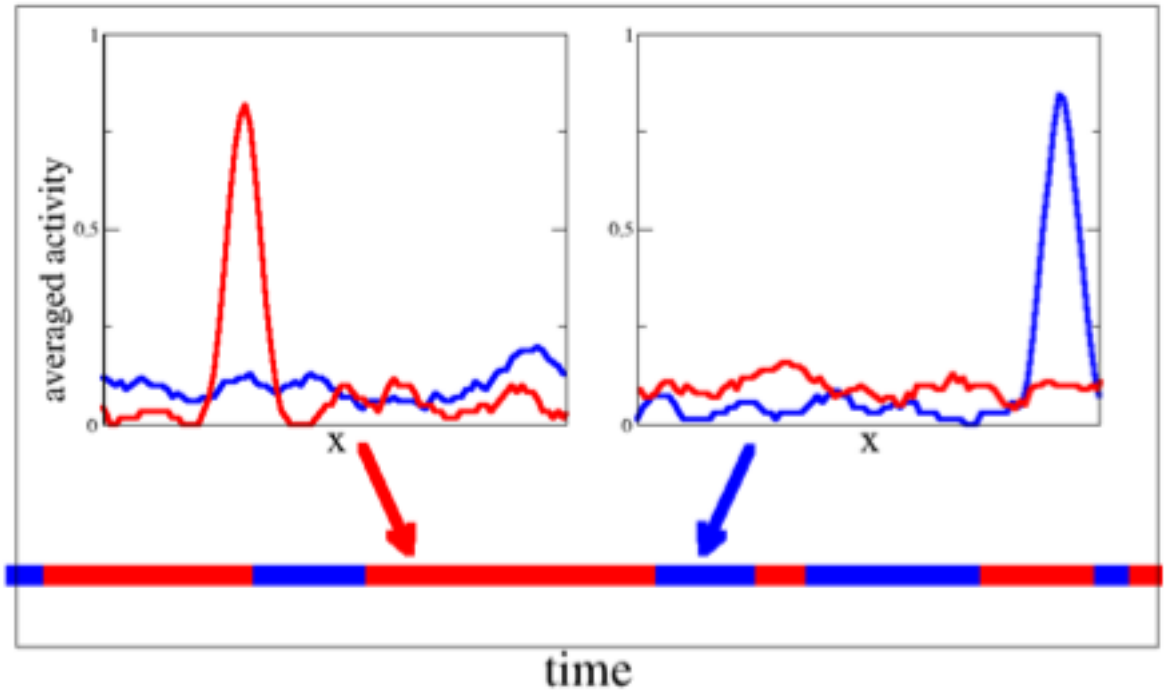


- Repeated transitions allow us to determine effective barrier heights and transition times:

$$\tau \approx e^{Nb(1\rightarrow 2)}$$

- Transitions take place at preferred locations in space(s)

# Conclusion & Perspectives

Storage of an extensive number of spatial charts in an attractor neural network…

… very robust to neural noise (temperature) !

$$H = -\sum_{i<j}\sum_{l} J^{0}_{\pi^l(i),\pi^l(j)}\sigma_i\sigma_j$$

$$H = -\sum_{i<j}\left(\sum_{\mu}\xi_i^{\mu}\xi_j^{\mu}\right)\sigma_i\sigma_j$$

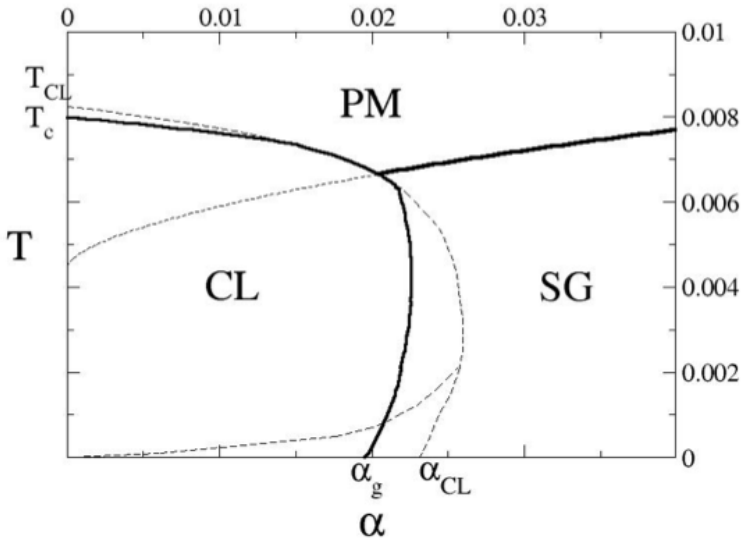


vs.

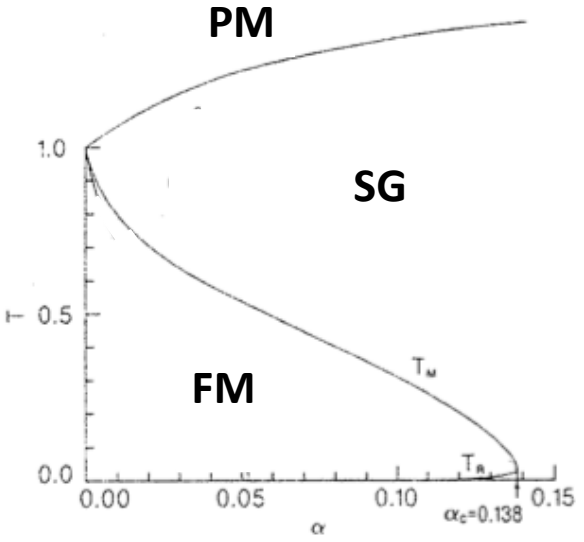


Amit, Gutfreund, Sompolinsky (1984)

# Conclusion & Perspectives

Complete picture of the dynamics within and between charts?

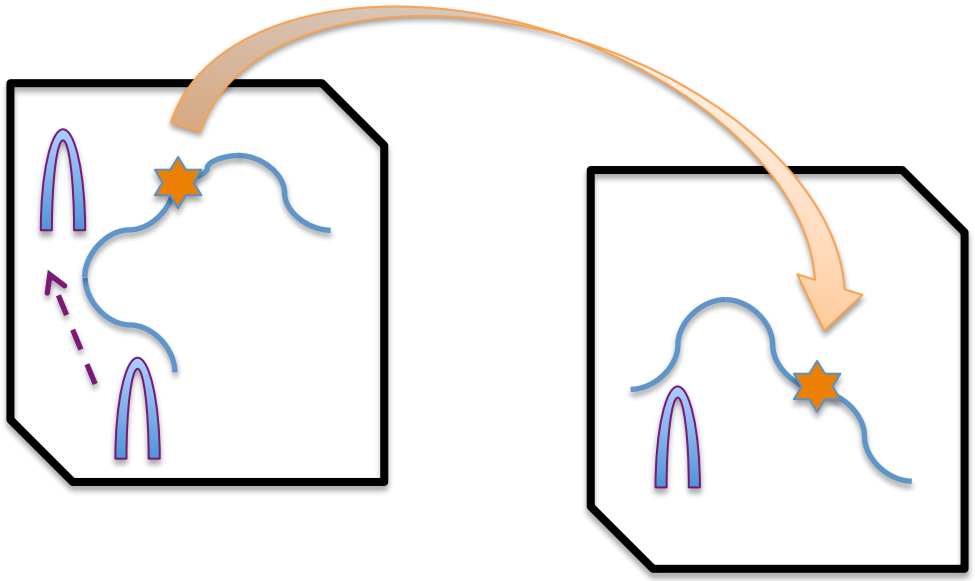

Competition between (activated) diffusion and transitions …
Depends on N (or effective N)
How to enhance diffusion in disordered landscape?
*(modulation of activity, orthogonalization of maps, adaptation, …)*

# Conclusion & Perspectives

Complete picture of the dynamics within and between charts?

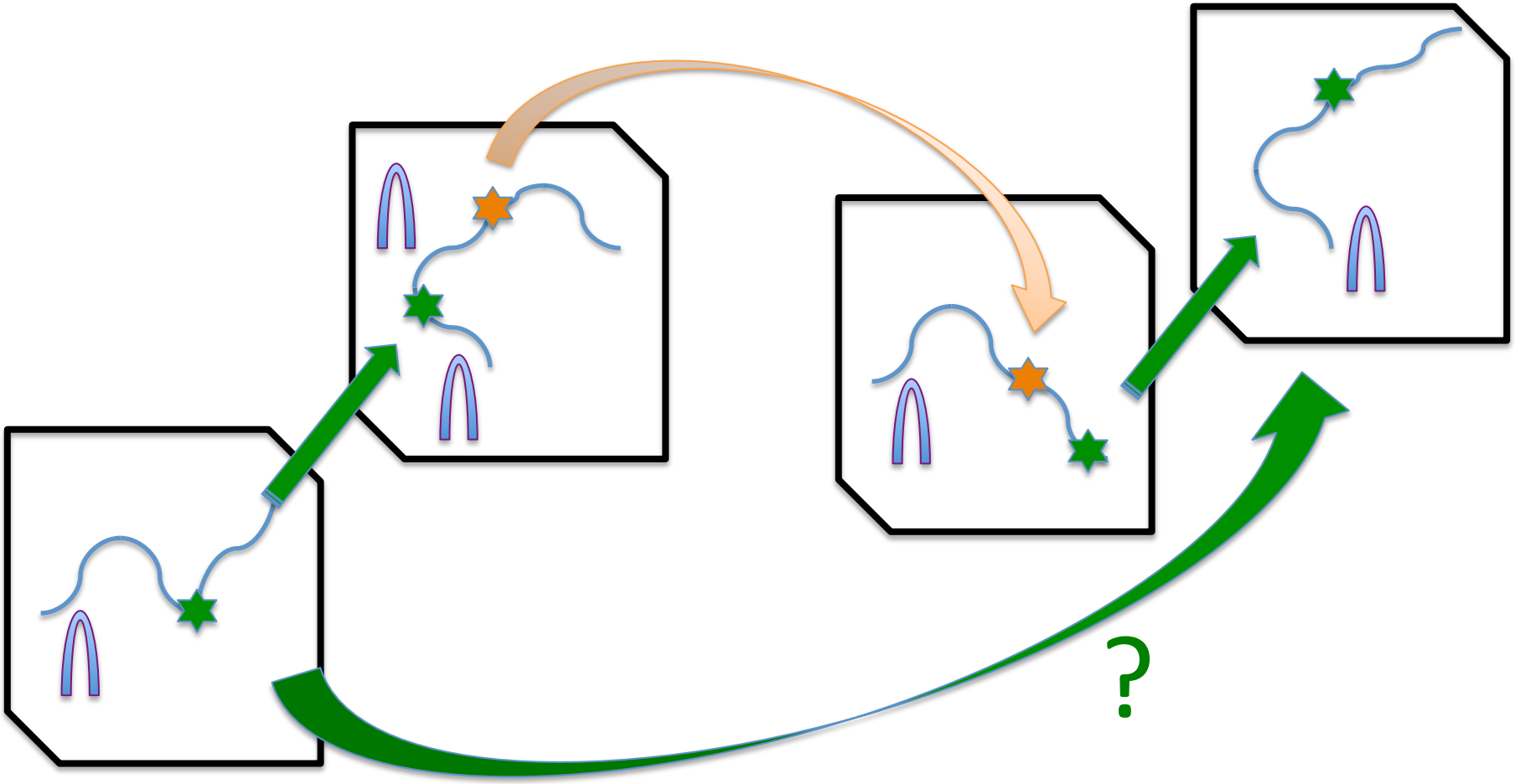

# Conclusion & Perspectives

Comparison/relationship with experiments:

- quantitative estimates of parameters in the model?
- specific locations for transitions?
- differences between D=1,2,3?
- dynamical behavior of clump under external forcing (visual clues)?
- extension to other spaces, context-dependent place fields?

# To go further

Some references:

F.P. Battaglia and A. Treves, Physical Review E 58, 7738 (1998).
M. Tsodyks, Hippocampus 9, 481 (1999).
J.J. Hopfield, Proceedings of the National Academy of Sciences 107, 1648 (2010).

Our paper: R.M., S. Rosay, Physical Review E 87, 062813 (2013) *(equilibrium only)*

and **Synopsis in Physics**, Knowing your Place, by D. Voss (http://physics.aps.org/)

Experiments: A Sense of Where You Are, New York Times, April 30th, 2013

# Post-doc available at Ecole Normale Supérieure, Paris

in collaboration with S. Cocco, M. Weigt and R.M.
Starting date: Fall 2014 at the latest

« From sequences to structure: statistical-physics methods to infer co-evolutionary constraints in proteins and RNAs »

- *Statistical physics of disordered systems*
- *Inverse problems*
- *Applications to genomics & homology detection*

See lectures by M. Weigt